
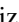
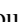




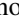
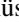
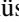
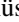







Search for Multimessenger Sources of Gravitational Waves and High-energy Neutrinos with Advanced LIGO during Its First Observing Run, ANTARES, and IceCube

A. Albert¹, M. André², M. Anghinolfi³, M. Ardid⁴, J.-J. Aubert⁵, J. Aublin⁶, T. Avgitas⁶, B. Baret⁶ , J. Barrios-Martí⁷, S. Basa⁸, B. Belhorma⁹, V. Bertin⁵, S. Biagi¹⁰, R. Bormuth^{11,12}, J. Boumaaza¹³, S. Bourret⁶, M. C. Bouwhuis¹¹, H. Brânzaș¹⁴, R. Bruijn^{11,15}, J. Brunner⁵, J. Busto⁵, A. Capone^{16,17}, L. Caramete¹⁴, J. Carr⁵, S. Celli^{16,17,18}, M. Chabab¹⁹, R. Cherkaoui El Moursli¹³, T. Chiarusi²⁰, M. Circella²³, J. A. B. Coelho⁶, A. Coleiro^{6,7}, M. Colomer^{6,7}, R. Coniglione¹⁰, H. Costantini⁵, P. Coyle⁵, A. Creusot⁶, A. F. Díaz²², A. Deschamps²³, C. Distefano¹⁰, I. Di Palma^{16,17}, A. Domi^{3,24}, R. Donà²⁰, C. Donzaud⁷, D. Dornic⁵, D. Drouhin¹, T. Eberl²⁶, I. El Bojaddaini²⁷, N. El Khayati¹³, D. Elsässer²⁸, A. Enzenhöfer^{5,26}, A. Ettahiri¹³, F. Fassi¹³, I. Felis⁴, P. Fermani^{16,17}, G. Ferrara¹⁰, L. Fusco^{6,29}, P. Gay^{6,30}, H. Glotin³¹, T. Grégoire⁶ , R. Gracia Ruiz¹, K. Graf²⁶, S. Hallmann²⁶, H. van Haren³², A. J. Heijboer¹¹, Y. Hello²³, J. J. Hernández-Rey⁷, J. Höbbl²⁶, J. Hofestädt²⁶, G. Illuminati⁷, M. de Jong^{11,12}, M. Jongen¹¹, M. Kadler²⁸ , O. Kalekin²⁶ , U. Katz²⁶ , N. R. Khan-Chowdhury⁷, A. Kouchner^{6,33}, M. Kreter²⁸, I. Kreykenbohm³⁴, V. Kulikovskiy^{3,35}, C. Lachaud⁶, R. Lahmann²⁶, D. Lefèvre^{36,37}, E. Leonora³⁸ , G. Levi^{20,29}, M. Lotze⁷, S. Loucatos^{6,39}, G. Maggi⁵, M. Marcellin⁸, A. Margiotta^{20,29}, A. Marinelli^{40,41} , J. A. Martínez-Mora⁴, R. Mele^{42,43} , K. Melis^{11,15}, P. Migliozzi⁴² , A. Moussa²⁷, S. Navas⁴⁴, E. Nezzi⁸, A. Nuñez^{5,8}, M. Organokov¹, G. E. Pávlaș¹⁴, C. Pellegrino^{20,29}, P. Piattelli¹⁰, V. Popa¹⁴, T. Pradier¹, L. Quinn⁵, C. Racca⁴⁵, N. Randazzo³⁸, G. Riccobene¹⁰, A. Sánchez-Losa²¹, M. Saldaña⁴, I. Salvadori⁵, D. F. E. Samtleben^{11,12}, M. Sanguineti^{3,24} , P. Sapienza¹⁰, F. Schüssler³⁹, M. Spurio^{20,29} , Th. Stolarczyk³⁹ , M. Taiuti^{3,24}, Y. Tayalati¹³, A. Trovato¹⁰, B. Vallage^{6,39}, V. Van Elewyck^{6,33} , F. Versari^{20,29}, D. Vivolo^{42,43}, J. Wilms³⁴ , D. Zaborov⁵, J. D. Zornoza⁷, J. Zúñiga⁷

(ANTARES collaboration),

M. G. Aartsen⁴⁶, M. Ackermann⁴⁷, J. Adams⁴⁶, J. A. Aguilar⁴⁸, M. Ahlers⁴⁹ , M. Ahrens⁵⁰, D. Altmann⁵¹, K. Andeen⁵², T. Anderson⁵³, I. Ansseau⁴⁸, G. Anton⁵¹, C. Argüelles⁵⁴, J. Auffenberg⁵⁵, S. Axani⁵⁴, P. Backes⁵⁵, H. Bagherpour⁴⁶, X. Bai⁵⁶, A. Barbano⁵⁷, J. P. Barron⁵⁸, S. W. Barwick⁵⁹, V. Baum⁶⁰, R. Bay⁶¹, J. J. Beatty^{62,63}, J. Becker Tjus⁶⁴, K.-H. Becker⁶⁵, S. BenZvi⁶⁶, D. Berley⁶⁷, E. Bernardini⁴⁷ , D. Z. Besson⁶⁸, G. Binder⁶⁹, D. Bindig⁶⁵, E. Blaufuss⁶⁷, S. Blot⁴⁷, C. Bohm⁵⁰, M. Börner⁷⁰, F. Bos⁶⁴, S. Böser⁶⁰, O. Botner⁷¹, E. Bourbeau⁴⁹, J. Bourbeau⁷², F. Bradascio⁴⁷, J. Braun⁷², M. Brenzke⁵⁵, H.-P. Bretz⁴⁷, S. Bron⁵⁷, J. Brostean-Kaiser⁴⁷, A. Burgman⁷¹, R. S. Busse⁷², T. Carver⁵⁷, E. Cheung⁶⁷, D. Chirkin⁷², K. Clark⁷³, L. Classen⁷⁴, G. H. Collin⁵⁴, J. M. Conrad⁵⁴, P. Coppin⁷⁵, P. Correa⁷⁵, D. F. Cowen^{53,76}, R. Cross⁶⁶, P. Dave⁷⁷, M. Day⁷², J. P. A. M. de André⁷⁸, C. De Clercq⁷⁵, J. J. DeLaunay⁵³ , H. Dembinski⁷⁹, K. Deoskar⁸⁰, S. De Ridder⁸⁰, P. Desiati⁷² , K. D. de Vries⁷⁵, G. de Wasseige⁷⁵ , M. de With⁸¹, T. DeYoung⁷⁸, J. C. Díaz-Vélez⁷², V. di Lorenzo⁶⁰, H. Dujmovic⁸², J. P. Dumm⁵⁰, M. Dunkman⁵³, E. Dvorak⁵⁶, B. Eberhardt², T. Ehrhardt⁶⁰, B. Eichmann⁶⁴, P. Eller⁵³, P. A. Evenson⁷⁹ , S. Fahey⁷², A. R. Fazely⁸³, J. Felde⁶⁷, K. Filimonov⁶¹, C. Finley⁵⁰, A. Franckowiak⁴⁷ , E. Friedman⁶⁷, A. Fritz⁶⁰, T. K. Gaisser⁷⁹, J. Gallagher⁸⁴ , E. Ganster⁵⁵, S. Garrappa⁴⁷, L. Gerhardt⁶⁹, K. Ghorbani⁷², W. Giang⁵⁸, T. Glauch⁸⁵, T. Glüsenkamp⁵¹ , A. Goldschmidt⁶⁹, J. G. Gonzalez⁷⁹, D. Grant⁵⁸, Z. Griffith⁷², C. Haack⁵⁵, A. Hallgren⁷¹, L. Halve⁵⁵, F. Halzen⁷², K. Hanson⁷², D. Hebecker⁸¹, D. Heereman⁴⁸, K. Helbing⁶⁵, R. Hellauer⁶⁷, S. Hickford⁶⁵, J. Hignight⁷⁸, G. C. Hill⁸⁶, K. D. Hoffman⁶⁷, R. Hoffmann⁶⁵, T. Hoinka⁷⁰, B. Hokanson-Fasig⁷², K. Hoshina^{72,87}, F. Huang⁵³, M. Huber⁸⁵ , K. Hultqvist⁵⁰, M. Hünnefeld⁷⁰, R. Hussain⁷², S. In⁸², N. Iovine⁴⁸, A. Ishihara⁸⁸, E. Jacobi⁴⁷, G. S. Japaridze⁸⁹, M. Jeong⁸², K. Jero⁷², B. J. P. Jones⁹⁰, P. Kalaczynski⁵⁵, W. Kang⁸², A. Kappes⁷⁴, D. Kappesser⁶⁰, T. Karg⁴⁷, A. Karle⁷², M. Kauer⁷², A. Keivani⁵³ , J. L. Kelley⁷², A. Kheirandish⁷², J. Kim⁸², T. Kintscher⁴⁷, J. Kiryluk⁹¹, T. Kittler⁵¹, S. R. Klein^{61,69}, R. Koirala⁷⁹, H. Kolanoski⁸¹, L. Köpke⁶⁰, C. Kopper⁵⁸, S. Kopper⁹², J. P. Koschinsky⁵⁵, D. J. Koskinen⁴⁹, M. Kowalski^{47,81}, K. Krings⁸⁵, M. Kroll⁶⁴, G. Krückl⁶⁰, S. Kunwar⁴⁷, N. Kurahashi⁹³, A. Kyriacou⁸⁶, M. Labare⁸⁰, J. L. Lanfranchi⁵³, M. J. Larson⁴⁹, F. Lauber⁶⁵, K. Leonard⁷², M. Leuermann⁵⁵, Q. R. Liu⁷², E. Lohfink⁶⁰, C. J. Lozano Mariscal⁷⁴, L. Lu⁸⁸, J. Lünemann⁷⁵, W. Luszczak⁷², J. Madsen⁹⁴, G. Maggi⁷⁵, K. B. M. Mahn⁷⁸, Y. Makino⁸⁸, S. Mancina⁷², I. C. Mariş⁴⁸, R. Maruyama⁹⁵, K. Mase⁸⁸, R. Maunu⁶⁷, K. Meagher⁴⁸, M. Medici⁴⁹, M. Meier⁷⁰, T. Menne⁷⁰, G. Merino⁷², T. Meures⁴⁸, S. Miarecki^{61,69}, J. Micallef⁷⁸, G. Momenti⁶⁰, T. Montaruli⁵⁷, R. W. Moore⁵⁸, M. Moulai⁵⁴, R. Nagai⁸⁸, R. Nahnhauser⁴⁷, P. Nakarmi⁹², U. Naumann⁶⁵, G. Neer⁷⁸, H. Niederhausen⁹¹, S. C. Nowicki⁵⁸, D. R. Nygren⁶⁹, A. Obertacke Pollmann⁶⁵, A. Olivas⁶⁷, A. O'Murchadha⁴⁸, E. O'Sullivan⁵⁰, T. Palczewski^{61,69}, H. Pandya⁷⁹, D. V. Pankova⁵³, P. Peiffer⁶⁰, J. A. Pepper⁹², C. Pérez de los Heros⁷¹, D. Pieloth⁷⁰, E. Pinat⁴⁸, A. Pizzuto⁷², M. Plum⁵², P. B. Price⁶¹, G. T. Przybylski⁶⁹, C. Raab⁴⁸, M. Rameez⁴⁹, L. Rauch⁴⁷, K. Rawlins⁹⁶, I. C. Rea⁸⁵, R. Reimann⁵⁵, B. Relethford⁹³, G. Renzi⁴⁸, E. Resconi⁸⁵, W. Rhode⁷⁰, M. Richman⁹³, S. Robertson⁶⁹, M. Rongen⁵⁵, C. Rott⁸², T. Ruhe⁷⁰, D. Ryckbosch⁸⁰, D. Rysewyk⁷⁸, I. Safa⁷², S. E. Sanchez Herrera⁵⁸, A. Sandrock⁷⁰, J. Sandroos⁶⁰, M. Santander⁹² , S. Sarkar^{49,97}, S. Sarkar⁵⁸, K. Satalecka⁴⁷, M. Schaufel⁵⁵, P. Schlunder⁷⁰, T. Schmidt⁶⁷, A. Schneider⁷², J. Schneider⁵¹, S. Schöneberg⁶⁴, L. Schumacher⁵⁵, S. Sclafani⁹³, D. Seckel⁷⁹, S. Seunarine⁹⁴, J. Soedingrekso⁷⁰, D. Soldin⁷⁹, M. Song⁶⁷, G. M. Spiczak⁹⁴, C. Spiering⁴⁷, J. Stachurska⁴⁷, M. Stamatikos⁶², T. Stanev⁷⁹, A. Stasik⁴⁷, R. Stein⁴⁷, J. Stettner⁵⁵, A. Steuer⁶⁰, T. Stezelberger⁶⁹, R. G. Stokstad⁶⁹, A. Stößl⁸⁸, N. L. Strotjohann⁴⁷, T. Stuttard⁴⁹, G. W. Sullivan⁶⁷, M. Sutherland⁶², I. Taboada⁷⁷, F. Tenholt⁶⁴, S. Ter-Antonyan⁸³, A. Terliuk⁴⁷, S. Tilav⁷⁹, P. A. Toale⁹², M. N. Tobin⁷², C. Tönnis⁸², S. Toscano⁷⁵, D. Tosi⁷², M. Tselengidou⁵¹, C. F. Tung⁷⁷, A. Turcati⁸⁵, R. Turcotte⁵⁵, C. F. Turley⁵³, B. Ty⁷², E. Unger⁷¹, M. A. Unland Elorrieta⁷⁴, M. Usner⁴⁷

J. Vandenbroucke⁷², W. Van Driessche⁸⁰, D. van Eijk⁷², N. van Eijndhoven⁷⁵, S. Vanheule⁸⁰, J. van Santen⁴⁷, M. Vraeghe⁸⁰,
 C. Walck⁵⁰, A. Wallace⁸⁶, M. Wallraff⁵⁵, F. D. Wandler⁵⁸, N. Wandkowsky⁷², T. B. Watson⁹⁰, A. Waza⁵⁵, C. Weaver⁵⁸,
 M. J. Weiss⁵³, C. Wendt⁷², J. Werthebach⁷², S. Westerhoff⁷², B. J. Whelan⁸⁶, N. Whitehorn⁹⁸, K. Wiebe⁶⁰, C. H. Wiebusch⁵⁵,
 L. Wille⁷², D. R. Williams⁹², L. Wills⁹³, M. Wolf⁸⁵, J. Wood⁷², T. R. Wood⁵⁸, E. Woolsey⁵⁸, K. Woschnagg⁶¹, G. Wrede⁵¹,
 D. L. Xu⁷², X. W. Xu⁸³, Y. Xu⁹¹, J. P. Yanez⁵⁸, G. Yodh⁵⁹, S. Yoshida⁸⁸, T. Yuan⁷²

(IceCube Collaboration),

and

B. P. Abbott⁹⁹, R. Abbott⁹⁹, T. D. Abbott¹⁰⁰, S. Abraham¹⁰¹, F. Acernese^{102,103}, K. Ackley¹⁰⁴, C. Adams¹⁰⁵, V. B. Adya^{106,107},
 C. Affeldt^{106,107}, M. Agathos¹⁰⁸, K. Agatsuma¹⁰⁹, N. Aggarwal¹¹⁰, O. D. Aguiar¹¹¹, L. Aiello^{112,113}, A. Ain¹⁰¹, P. Ajith¹¹⁴,
 G. Allen¹¹⁵, A. Allocca^{116,117}, M. A. Aloy¹¹⁸, P. A. Altin¹¹⁹, A. Amato¹²⁰, A. Ananyeva⁹⁹, S. B. Anderson⁹⁹, W. G. Anderson¹²¹,
 S. V. Angelova¹²², S. Antier¹²³, S. Appert⁹⁹, K. Arai⁹⁹, M. C. Araya⁹⁹, J. S. Areeda¹²⁴, M. Arène¹²⁵, N. Arnaud^{123,126},
 K. G. Arun¹²⁷, S. Ascenzi^{128,129}, G. Ashton¹⁰⁴, S. M. Aston¹⁰⁵, P. Astone¹³⁰, F. Aubin¹³¹, P. Aufmuth¹⁰⁷, K. AultONeal¹³²,
 C. Austin¹⁰⁰, V. Avendano¹³³, A. Avila-Alvarez¹²⁴, S. Babak^{125,134}, P. Bacon¹²⁵, F. Badaracco^{112,113}, M. K. M. Bader¹³⁵,
 S. Bae¹³⁶, P. T. Baker¹³⁷, F. Baldaccini^{138,139}, G. Ballardín¹²⁶, S. W. Ballmer¹⁴⁰, S. Banagiri¹⁴¹, J. C. Barayoga⁹⁹, S. E. Barclay¹⁴²,
 B. C. Barish⁹⁹, D. Barker¹⁴³, K. Barkett¹⁴⁴, S. Barnum¹¹⁰, F. Barone^{102,103}, B. Barr¹⁴², L. Barsotti¹¹⁰, M. Barsuglia¹²⁵, D. Barta¹⁴⁵,
 J. Bartlett¹⁴³, I. Bartos¹⁴⁶, R. Bassiri¹⁴⁷, A. Basti^{116,117}, M. Bawaj^{139,148}, J. C. Bayley¹⁴², M. Bazzan^{149,150}, B. Bécsy¹⁵¹,
 M. Bejger^{125,152}, I. Belahcene¹²³, A. S. Bell¹⁴², D. Beniwal¹⁵³, B. K. Berger¹⁴⁷, G. Bergmann^{106,107}, S. Bernuzzi^{154,155},
 J. J. Bero¹⁵⁶, C. P. L. Berry¹⁵⁷, D. Bersanetti¹⁵⁸, A. Bertolini¹³⁵, J. Betzwieser¹⁰⁵, R. Bhandare¹⁵⁹, J. Bidler¹²⁴, I. A. Bilenko¹⁶⁰,
 S. A. Bilgili¹³⁷, G. Billingsley⁹⁹, J. Birch¹⁰⁵, R. Birney¹²², O. Birnholtz¹⁵⁶, S. Biscans^{99,110}, S. Biscoveanu¹⁰⁴, A. Bisht¹⁰⁷,
 M. Bitossi^{117,126}, M. A. Bizouard¹²³, J. K. Blackburn⁹⁹, C. D. Blair¹⁰⁵, D. G. Blair¹⁶¹, R. M. Blair¹⁴³, S. Bloemen¹⁶²,
 N. Bode^{106,107}, M. Boer¹⁶³, Y. Boetzel¹⁶⁴, G. Bogaert¹⁶³, F. Bondu¹⁶⁵, E. Bonilla¹⁴⁷, R. Bonnand¹³¹, P. Booker^{106,107},
 B. A. Boom¹³⁵, C. D. Booth¹⁶⁶, R. Bork⁹⁹, V. Boschi¹²⁶, S. Bose^{101,167}, K. Bossie¹⁰⁵, V. Bossilkov¹⁶¹, J. Bosveld¹⁶¹,
 Y. Bouffanais¹²⁵, A. Bozzi¹²⁶, C. Bradaschia¹¹⁷, P. R. Brady¹²¹, A. Bramley¹⁰⁵, M. Branchesi^{112,113}, J. E. Brau¹⁶⁸, T. Briant¹⁶⁹,
 J. H. Briggs¹⁴², F. Brighenti^{170,171}, A. Brillet¹⁶³, M. Brinkmann^{106,107}, V. Brisson^{123,272}, P. Brockill¹²¹, A. F. Brooks⁹⁹,
 D. D. Brown¹⁵³, S. Brunett⁹⁹, A. Buikema¹¹⁰, T. Bulik¹⁷², H. J. Bulten^{135,173}, A. Buonanno^{134,174}, D. Buskulic¹³¹, C. Buy¹²⁵,
 R. L. Byer¹⁴⁷, M. Cabero^{106,107}, L. Cadonati¹⁷⁵, G. Cagnoli^{120,176}, C. Cahillane⁹⁹, J. Calderón Bustillo¹⁰⁴, T. A. Callister⁹⁹,
 E. Calloni^{103,177}, J. B. Camp¹⁷⁸, W. A. Campbell¹⁰⁴, K. C. Cannon¹⁷⁹, H. Cao¹⁵³, J. Cao¹⁸⁰, E. Capocasa¹²⁵, F. Carbognani¹²⁶,
 S. Caride¹⁸¹, M. F. Carney¹⁵⁷, G. Carullo¹¹⁶, J. Casanueva Diaz¹¹⁷, C. Casentini^{128,129}, S. Caudill¹³⁵, M. Cavaglia¹⁸²,
 F. Cavalier¹²³, R. Cavalieri¹²⁶, G. Cella¹¹⁷, P. Cerdá-Durán¹¹⁸, G. Cerretani^{116,117}, E. Cesarini^{129,183}, O. Chaibi¹⁶³,
 K. Chakravarti¹⁰¹, S. J. Chamberlin¹⁸⁴, M. Chan¹⁴², S. Chao¹⁸⁵, P. Charlton¹⁸⁶, E. A. Chase¹⁵⁷, E. Chassande-Mottin¹²⁵,
 D. Chatterjee¹²¹, M. Chaturvedi¹⁵⁹, B. D. Cheeseboro¹³⁷, H. Y. Chen¹⁸⁷, X. Chen¹⁶¹, Y. Chen¹⁴⁴, H.-P. Cheng¹⁴⁶, C. K. Cheong¹⁸⁸,
 H. Y. Chia¹⁴⁶, A. Chincarini¹⁵⁸, A. Chiummo¹²⁶, G. Cho¹⁸⁹, H. S. Cho¹⁹⁰, M. Cho¹⁷⁴, N. Christensen^{163,191}, Q. Chu¹⁶¹, S. Chua¹⁶⁹,
 K. W. Chung¹⁸⁸, S. Chung¹⁶¹, G. Ciani^{149,150}, A. A. Ciobanu¹⁵³, R. Ciolfi^{192,193}, F. Cipriano¹⁶³, A. Cirone^{158,194}, F. Clara¹⁴³,
 J. A. Clark¹⁷⁵, P. Clearwater¹⁹⁵, F. Cleva¹⁶³, C. Cocchieri¹⁸², E. Coccia^{112,113}, P.-F. Cohadon¹⁶⁹, D. Cohen¹²³, R. Colgan¹⁹⁶,
 M. Colleoni¹⁹⁷, C. G. Collette¹⁹⁸, C. Collins¹⁰⁹, L. R. Cominsky¹⁹⁹, M. Constanancio, Jr.¹¹¹, L. Conti¹⁵⁰, S. J. Cooper¹⁰⁹,
 P. Corban¹⁰⁵, T. R. Corbitt¹⁰⁰, I. Cordero-Carrión²⁰⁰, K. R. Corley¹⁹⁶, N. Cornish²⁰¹, A. Corsi¹⁸¹, S. Cortese¹²⁶,
 C. A. Costa¹¹¹, R. Cotesta¹³⁴, M. W. Coughlin⁹⁹, S. B. Coughlin^{157,166}, J.-P. Coulon¹⁶³, S. T. Countryman¹⁹⁶, P. Couvares⁹⁹,
 P. B. Covas¹⁹⁷, E. E. Cowan¹⁷⁵, D. M. Coward¹⁶¹, M. J. Cowart¹⁰⁵, D. C. Coyne⁹⁹, R. Coyne²⁰², J. D. E. Creighton¹²¹,
 T. D. Creighton²⁰³, J. Cripe¹⁰⁰, M. Croquette¹⁶⁹, S. G. Crowder²⁰⁴, T. J. Cullen¹⁰⁰, A. Cumming¹⁴², L. Cunningham¹⁴²,
 E. Cuoco¹²⁶, T. Dal Canton¹⁷⁸, G. Dálya¹⁵¹, S. L. Danilishin^{106,107}, S. D'Antonio¹²⁹, K. Danzmann^{106,107}, A. Dasgupta²⁰⁵,
 C. F. Da Silva Costa¹⁴⁶, L. E. H. Datrier¹⁴², V. Dattilo¹²⁶, I. Dave¹⁵⁹, M. Davier¹²³, D. Davis¹⁴⁰, E. J. Daw²⁰⁶, D. DeBra¹⁴⁷,
 M. Deenadayalan¹⁰¹, J. Degallaix¹²⁰, M. De Laurentis^{103,177}, S. Deléglise¹⁶⁹, W. Del Pozzo^{116,117}, L. M. DeMarchi¹⁵⁷,
 N. Demos¹¹⁰, T. Dent^{106,107}, M. Denys¹⁷², R. De Pietri^{155,207}, J. Derby¹²⁴, R. De Rosa^{103,177}, C. De Rossi^{120,126}, R. DeSalvo²⁰⁸,
 O. de Varona^{106,107}, S. Dhurandhar¹⁰¹, M. C. Díaz²⁰³, T. Dietrich¹³⁵, L. Di Fiore¹⁰³, M. Di Giovanni^{193,209}, T. Di Girolamo^{103,177},
 A. Di Lieto^{116,117}, B. Ding¹⁹⁸, S. Di Pace^{130,210}, F. Di Renzo^{116,117}, A. Dmitriev¹⁰⁹, Z. Doctor¹⁸⁷, F. Donovan¹¹⁰,
 K. L. Dooley^{166,182}, S. Doravari^{106,107}, I. Dorrington¹⁶⁶, T. P. Downes¹²¹, M. Drago^{112,113}, J. C. Driggers¹⁴³, Z. Du¹⁸⁰,
 J.-G. Ducoin¹²³, P. Dupej¹⁴², S. E. Dwyer¹⁴³, P. J. Easter¹⁰⁴, T. B. Edo²⁰⁶, M. C. Edwards¹⁹¹, A. Effler¹⁰⁵, P. Ehrens⁹⁹,
 J. Eichholz⁹⁹, S. S. Eikenberry¹⁴⁶, M. Eisenmann¹³¹, R. A. Eisenstein¹¹⁰, R. C. Essick¹⁸⁷, H. Estelles¹⁹⁷, D. Estevez¹³¹,
 Z. B. Etienne¹³⁷, T. Etzel⁹⁹, M. Evans¹¹⁰, T. M. Evans¹⁰⁵, V. Fafone^{112,128,129}, H. Fair¹⁴⁰, S. Fairhurst¹⁶⁶, X. Fan¹⁸⁰,
 S. Farinon¹⁵⁸, B. Farr¹⁶⁸, W. M. Farr¹⁰⁹, E. J. Fauchon-Jones¹⁶⁶, M. Favata¹³³, M. Fays²⁰⁶, M. Fazio²¹¹, C. Fee²¹², J. Feicht⁹⁹,
 M. M. Fejer¹⁴⁷, F. Feng¹²⁵, A. Fernandez-Galiana¹¹⁰, I. Ferrante^{116,117}, E. C. Ferreira¹¹¹, T. A. Ferreira¹¹¹, F. Ferrini¹²⁶,
 F. Fidecaro^{116,117}, I. Fiori¹²⁶, D. Fiorucci¹²⁵, M. Fishbach¹⁸⁷, R. P. Fisher^{140,213}, J. M. Fishner¹¹⁰, M. Fitz-Axen¹⁴¹,
 R. Flamini^{131,214}, M. Fletcher¹⁴², E. Flynn¹²⁴, H. Fong²¹⁵, J. A. Font^{118,216}, P. W. F. Forsyth¹¹⁹, J.-D. Fournier¹⁶³, S. Frasca^{130,210},
 F. Frasconi¹¹⁷, Z. Frei¹⁵¹, A. Freise¹⁰⁹, R. Frey¹⁶⁸, V. Frey¹²³, P. Fritschel¹¹⁰, V. V. Frolov¹⁰⁵, P. Fulda¹⁴⁶, M. Fyffe¹⁰⁵,
 H. A. Gabbard¹⁴², B. U. Gadre¹⁰¹, S. M. Gaebel¹⁰⁹, J. R. Gair²¹⁷, L. Gammaitoni¹³⁸, M. R. Ganija¹⁵³, S. G. Gaonkar¹⁰¹,
 A. Garcia¹²⁴, C. García-Quirós¹⁹⁷, F. Garufi^{103,177}, B. Gateley¹⁴³, S. Gaudio¹³², G. Gaur²¹⁸, V. Gayathri²¹⁹, G. Gemme¹⁵⁸,
 E. Genin¹²⁶, A. Gennai¹¹⁷, D. George¹¹⁵, J. George¹⁵⁹, L. Gergely²²⁰, V. Germain¹³¹, S. Ghonge¹⁷⁵, Abhirup Ghosh¹¹⁴,

Archisman Ghosh¹³⁵, S. Ghosh¹²¹, B. Giacomazzo^{193,209}, J. A. Giaime^{100,105}, K. D. Giardino¹⁰⁵, A. Giazotto^{117,273}, K. Gill¹³², G. Giordano^{102,103}, L. Glover²⁰⁸, P. Godwin¹⁸⁴, E. Goetz¹⁴³, R. Goetz¹⁴⁶, B. Goncharov¹⁰⁴, G. González¹⁰⁰, J. M. Gonzalez Castro^{116,117}, A. Gopakumar²²¹, M. L. Gorodetsky¹⁶⁰, S. E. Gossan⁹⁹, M. Gosselin¹²⁶, R. Gouaty¹³¹, A. Grado^{103,222}, C. Graef¹⁴², M. Granata¹²⁰, A. Grant¹⁴², S. Gras¹¹⁰, P. Grassia⁹⁹, C. Gray¹⁴³, R. Gray¹⁴², G. Greco^{170,171}, A. C. Green^{109,146}, R. Green¹⁶⁶, E. M. Gretarsson¹³², P. Groot¹⁶², H. Grote¹⁶⁶, S. Grunewald¹³⁴, P. Gruning¹²³, G. M. Guidi^{170,171}, H. K. Gulati²⁰⁵, Y. Guo¹³⁵, A. Gupta¹⁸⁴, M. K. Gupta²⁰⁵, E. K. Gustafson⁹⁹, R. Gustafson²²³, L. Haegel¹⁹⁷, O. Halim^{112,113}, B. R. Hall¹⁶⁷, E. D. Hall¹¹⁰, E. Z. Hamilton¹⁶⁶, G. Hammond¹⁴², M. Haney¹⁶⁴, M. M. Hanke^{106,107}, J. Hanks¹⁴³, C. Hanna¹⁸⁴, O. A. Hannuksela¹⁸⁸, J. Hanson¹⁰⁵, T. Hardwick¹⁰⁰, K. Haris¹¹⁴, J. Harms^{112,113}, G. M. Harry²²⁴, I. W. Harry¹³⁴, C.-J. Haster²¹⁵, K. Haughian¹⁴², F. J. Hayes¹⁴², J. Healy¹⁵⁶, A. Heidmann¹⁶⁹, M. C. Heintze¹⁰⁵, H. Heitmann¹⁶³, P. Hello¹²³, G. Hemming¹²⁶, M. Hendry¹⁴², I. S. Heng¹⁴², J. Hennig^{106,107}, A. W. Heptonstall⁹⁹, F. J. Hernandez¹⁰⁴, M. Heurs^{106,107}, S. Hild¹⁴², T. Hinderer^{135,225,226}, D. Hoak¹²⁶, S. Hochheim^{106,107}, D. Hofman¹²⁰, A. M. Holgado¹¹⁵, N. A. Holland¹¹⁹, K. Holt¹⁰⁵, D. E. Holz¹⁸⁷, P. Hopkins¹⁶⁶, C. Horst¹²¹, J. Hough¹⁴², E. J. Howell¹⁶¹, C. G. Hoy¹⁶⁶, A. Hreibi¹⁶³, E. A. Huerta¹¹⁵, D. Huet¹²³, B. Hughey¹³², M. Hulko⁹⁹, S. Husa¹⁹⁷, S. H. Huttner¹⁴², T. Huynh-Dinh¹⁰⁵, B. Idzkowski¹⁷², A. Iess^{128,129}, C. Ingram¹⁵³, R. Inta¹⁸¹, G. Intini^{130,210}, B. Irwin²¹², H. N. Isa¹⁴², J.-M. Isac¹⁶⁹, M. Isi⁹⁹, B. R. Iyer¹¹⁴, K. Izumi¹⁴³, T. Jacqmin¹⁶⁹, S. J. Jadhav²²⁷, K. Jani¹⁷⁵, N. N. Jantihar²²⁷, P. Jaranowski²²⁸, A. C. Jenkins²²⁹, J. Jiang¹⁴⁶, D. S. Johnson¹¹⁵, A. W. Jones¹⁰⁹, D. I. Jones²³⁰, R. Jones¹⁴², R. J. G. Jonker¹³⁵, L. Ju¹⁶¹, J. Junker^{106,107}, C. V. Kalaghatgi¹⁶⁶, V. Kalogera¹⁵⁷, B. Kamai⁹⁹, S. Kandhasamy¹⁸², G. Kang¹³⁶, J. B. Kanner⁹⁹, S. J. Kapadia¹²¹, S. Karki¹⁶⁸, K. S. Karvinen^{106,107}, R. Kashyap¹¹⁴, M. Kasprzack⁹⁹, S. Katsanevas¹²⁶, E. Katsavounidis¹¹⁰, W. Katzman¹⁰⁵, S. Kaufer¹⁰⁷, K. Kawabe¹⁴³, N. V. Keerthana¹⁰¹, F. Kéfélian¹⁶³, D. Keitel¹⁴², R. Kennedy²⁰⁶, J. S. Key²³¹, F. Y. Khalili¹⁶⁰, H. Khan¹²⁴, I. Khan^{112,129}, S. Khan^{106,107}, Z. Khan²⁰⁵, E. A. Khazanov²³², M. Khurshed¹⁵⁹, N. Kijbunchoo¹¹⁹, Chunglee Kim²³³, J. C. Kim²³⁴, K. Kim¹⁸⁸, W. Kim¹⁵³, W. S. Kim²³⁵, Y.-M. Kim²³⁶, C. Kimball¹⁵⁷, E. J. King¹⁵³, P. J. King¹⁴³, M. Kinley-Hanlon²²⁴, R. Kirchhoff^{106,107}, J. S. Kissel¹⁴³, L. Kleybolte²³⁷, J. H. Klika¹²¹, S. Klimenko¹⁴⁶, T. D. Knowles¹³⁷, P. Koch^{106,107}, S. M. Koehlenbeck^{106,107}, G. Koekoek^{135,238}, S. Koley¹³⁵, V. Kondrashov⁹⁹, A. Kontos¹¹⁰, N. Koper^{106,107}, M. Korobko²³⁷, W. Z. Korth⁹⁹, I. Kowalska¹⁷², D. B. Kozak⁹⁹, V. Kringel^{106,107}, N. Krishnendu¹²⁷, A. Królak^{239,240}, G. Kuehn^{106,107}, A. Kumar²²⁷, P. Kumar²⁴¹, R. Kumar²⁰⁵, S. Kumar¹¹⁴, L. Kuo¹⁸⁵, A. Kutynia²³⁹, S. Kwang¹²¹, B. D. Lackey¹³⁴, K. H. Lai¹⁸⁸, T. L. Lam¹⁸⁸, M. Landry¹⁴³, B. B. Lane¹¹⁰, R. N. Lang²⁴², J. Lange¹⁵⁶, B. Lantz¹⁴⁷, R. K. Lanza¹¹⁰, A. Lartaux-Vollard¹²³, P. D. Lasky¹⁰⁴, M. Laxen¹⁰⁵, A. Lazzarini⁹⁹, C. Lazzaro¹⁵⁰, P. Leaci^{130,210}, S. Leavey^{106,107}, Y. K. Lecoecue¹⁴³, C. H. Lee¹⁹⁰, H. K. Lee²⁴³, H. M. Lee²⁴⁴, H. W. Lee²³⁴, J. Lee¹⁸⁹, K. Lee¹⁴², J. Lehmann^{106,107}, A. Lenon¹³⁷, N. Leroy¹²³, N. Letendre¹³¹, Y. Levin^{104,196}, J. Li¹⁸⁰, K. J. L. Li¹⁸⁸, T. G. F. Li¹⁸⁸, X. Li¹⁴⁴, F. Lin¹⁰⁴, F. Linde¹³⁵, S. D. Linker²⁰⁸, T. B. Littenberg²⁴⁵, J. Liu¹⁶¹, X. Liu¹²¹, R. K. L. Lo^{99,188}, N. A. Lockerbie¹²², L. T. London¹⁶⁶, A. Longo^{246,247}, M. Lorenzini^{112,113}, V. Lorette²⁴⁸, M. Lormand¹⁰⁵, G. Losurdo¹¹⁷, J. D. Lough^{106,107}, C. O. Lousto¹⁵⁶, G. Lovelace¹²⁴, M. E. Lower²⁴⁹, H. Lück^{106,107}, D. Lumaca^{128,129}, A. P. Lundgren²⁵⁰, R. Lynch¹¹⁰, Y. Ma¹⁴⁴, R. Macas¹⁶⁶, S. Macfoy¹²², M. MacInnis¹¹⁰, D. M. Macleod¹⁶⁶, A. Macquet¹⁶³, F. Magaña-Sandoval¹⁴⁰, L. Magaña Zertuche¹⁸², R. M. Magee¹⁸⁴, E. Majorana¹³⁰, I. Maksimovic²⁴⁸, A. Malik¹⁵⁹, N. Man¹⁶³, V. Mandic¹⁴¹, V. Mangano¹⁴², G. L. Mansell^{110,143}, M. Manske^{119,121}, M. Mantovani¹²⁶, F. Marchesoni^{139,148}, F. Marion¹³¹, S. Márka¹⁹⁶, Z. Márka¹⁹⁶, C. Markakis^{108,115}, A. S. Markosyan¹⁴⁷, A. Markowitz⁹⁹, E. Maros⁹⁹, A. Marquina²⁰⁰, S. Marsat¹³⁴, F. Martelli^{170,171}, I. W. Martin¹⁴², R. M. Martin¹³³, D. V. Martynov¹⁰⁹, K. Mason¹¹⁰, E. Massera²⁰⁶, A. Maserot¹³¹, T. J. Massinger⁹⁹, M. Masso-Reid¹⁴², S. Mastrogiovanni^{130,210}, A. Matas^{134,141}, F. Matichard^{99,110}, L. Matone¹⁹⁶, N. Mavalvala¹¹⁰, N. Mazumder¹⁶⁷, J. J. McCann¹⁶¹, R. McCarthy¹⁴³, D. E. McClelland¹¹⁹, S. McCormick¹⁰⁵, L. McCuller¹¹⁰, S. C. McGuire²⁵¹, J. McIver⁹⁹, D. J. McManus¹¹⁹, T. McRae¹¹⁹, S. T. McWilliams¹³⁷, D. Meacher¹⁸⁴, G. D. Meadors¹⁰⁴, M. Mehmet^{106,107}, A. K. Mehta¹¹⁴, J. Meidam¹³⁵, A. Melatos¹⁹⁵, G. Mendell¹⁴³, R. A. Mercer¹²¹, L. Mereni¹²⁰, E. L. Merilh¹⁴³, M. Merzougui¹⁶³, S. Meshkov⁹⁹, C. Messenger¹⁴², C. Messick¹⁸⁴, R. Metzdrorf¹⁶⁹, P. M. Meyers¹⁹⁵, H. Miao¹⁰⁹, C. Michel¹²⁰, H. Middleton¹⁹⁵, E. E. Mikhailov²⁵², L. Milano^{103,177}, A. L. Miller¹⁴⁶, A. Miller^{130,210}, M. Millhouse²⁰¹, J. C. Mills¹⁶⁶, M. C. Milovich-Goff²⁰⁸, O. Minazzoli^{163,253}, Y. Minenkov¹²⁹, A. Mishkin¹⁴⁶, C. Mishra²⁵⁴, T. Mistry²⁰⁶, S. Mitra¹⁰¹, V. P. Mitrofanov¹⁶⁰, G. Mitselmakher¹⁴⁶, R. Mittleman¹¹⁰, G. Mo¹⁹¹, D. Moffa²¹², K. Mogushi¹⁸², S. R. P. Mohapatra¹¹⁰, M. Montani^{170,171}, C. J. Moore¹⁰⁸, D. Moraru¹⁴³, G. Moreno¹⁴³, S. Morisaki¹⁷⁹, B. Mours¹³¹, C. M. Mow-Lowry¹⁰⁹, Arunava Mukherjee^{106,107}, D. Mukherjee¹²¹, S. Mukherjee²⁰³, N. Mukund¹⁰¹, A. Mullavey¹⁰⁵, J. Munch¹⁵³, E. A. Muñoz¹⁴⁰, M. Muratore¹³², P. G. Murray¹⁴², I. Nardecchia^{128,129}, L. Naticchioni^{130,210}, R. K. Nayak²⁵⁵, J. Neilson²⁰⁸, G. Nelemans^{135,162}, T. J. N. Nelson¹⁰⁵, M. Nery^{106,107}, A. Neunzert²²³, K. Y. Ng¹¹⁰, S. Ng¹⁵³, P. Nguyen¹⁶⁸, D. Nichols^{135,225}, S. Nissanke^{135,225}, F. Nocera¹²⁶, C. North¹⁶⁶, L. K. Nuttall²⁵⁰, M. Obergaulinger¹¹⁸, J. Oberling¹⁴³, B. D. O'Brien¹⁴⁶, G. D. O'Dea²⁰⁸, G. H. Ogini²⁵⁶, J. J. Oh²³⁵, S. H. Oh²³⁵, F. Ohme^{106,107}, H. Ohta¹⁷⁹, M. A. Okada¹¹¹, M. Oliver¹⁹⁷, P. Oppermann^{106,107}, Richard J. Oram¹⁰⁵, B. O'Reilly¹⁰⁵, R. G. Ormiston¹⁴¹, L. F. Ortega¹⁴⁶, R. O'Shaughnessy¹⁵⁶, S. Ossokine¹³⁴, D. J. Ottaway¹⁵³, H. Overmier¹⁰⁵, B. J. Owen¹⁸¹, A. E. Pace¹⁸⁴, G. Pagano^{116,117}, M. A. Page¹⁶¹, A. Pai²¹⁹, S. A. Pai¹⁵⁹, J. R. Palamos¹⁶⁸, O. Palashov²³², C. Palomba¹³⁰, A. Pal-Singh²³⁷, Huang-Wei Pan¹⁸⁵, B. Pang¹⁴⁴, P. T. H. Pang¹⁸⁸, C. Pankow¹⁵⁷, F. Pannarale^{130,210}, B. C. Pant¹⁵⁹, F. Paoletti¹¹⁷, A. Paoli¹²⁶, A. Parida¹⁰¹, W. Parker^{105,251}, D. Pascucci¹⁴², A. Pasqualetti¹²⁶, R. Passaquetti^{116,117}, D. Passuello¹¹⁷, M. Patil²⁴⁰, B. Patricelli^{116,117}, B. L. Pearlstone¹⁴², C. Pedersen¹⁶⁶, M. Pedraza⁹⁹, R. Pedurand^{120,257}, A. Pele¹⁰⁵, S. Penn²⁵⁸, C. J. Perez¹⁴³, A. Perreca^{193,209}, H. P. Pfeiffer^{134,215}, M. Phelps^{106,107}, K. S. Phukon¹⁰¹, O. J. Piccinni^{130,210}, M. Pichot¹⁶³, F. Piergiovanni^{170,171}, G. Pillant¹²⁶, L. Pinard¹²⁰, M. Pirello¹⁴³, M. Pitkin¹⁴², R. Poggiani^{116,117}, D. Y. T. Pong¹⁸⁸, S. Ponrathnam¹⁰¹, P. Popolizio¹²⁶, E. K. Porter¹²⁵

J. Powell²⁴⁹, A. K. Prajapati²⁰⁵, J. Prasad¹⁰¹, K. Prasai¹⁴⁷, R. Prasanna²²⁷, G. Pratten¹⁹⁷, T. Prestegard¹²¹, S. Privitera¹³⁴, G. A. Prodi^{193,209}, L. G. Prokhorov¹⁶⁰, O. Puncken^{106,107}, M. Punturo¹³⁹, P. Puppato¹³⁰, M. Pürrier¹³⁴, H. Qi¹²¹, V. Quetschke²⁰³, P. J. Quinonez¹³², E. A. Quintero⁹⁹, R. Quitzow-James¹⁶⁸, F. J. Raab¹⁴³, H. Radkins¹⁴³, N. Radulescu¹⁶³, P. Raffai¹⁵¹, S. Raja¹⁵⁹, C. Rajan¹⁵⁹, B. Rajbhandari¹⁸¹, M. Rakhmanov²⁰³, K. E. Ramirez²⁰³, A. Ramos-Buades¹⁹⁷, Javed Rana¹⁰¹, K. Rao¹⁵⁷, P. Rapagnani^{130,210}, V. Raymond¹⁶⁶, M. Razzano^{116,117}, J. Read¹²⁴, T. Regimbau¹³¹, L. Rei¹⁵⁸, S. Reid¹²², D. H. Reitze^{99,146}, W. Ren¹¹⁵, F. Ricci^{130,210}, C. J. Richardson¹³², J. W. Richardson⁹⁹, P. M. Ricker¹¹⁵, K. Riles²²³, M. Rizzo¹⁵⁷, N. A. Robertson^{99,142}, R. Robie¹⁴², F. Robinet¹²³, A. Rocchi¹²⁹, L. Rolland¹³¹, J. G. Rollins⁹⁹, V. J. Roma¹⁶⁸, M. Romanelli¹⁶⁵, R. Romano^{102,103}, C. L. Romel¹⁴³, J. H. Romie¹⁰⁵, K. Rose²¹², D. Rosińska^{152,259}, S. G. Rosofsky¹¹⁵, M. P. Ross²⁶⁰, S. Rowan¹⁴², A. Rüdiger^{106,107,274}, P. Ruggi¹²⁶, G. Rutins²⁶¹, K. Ryan¹⁴³, S. Sachdev⁹⁹, T. Sadecki¹⁴³, M. Sakellariadou²²⁹, L. Salconi¹²⁶, M. Saleem¹²⁷, A. Samajdar¹³⁵, L. Sammut¹⁰⁴, E. J. Sanchez⁹⁹, L. E. Sanchez⁹⁹, N. Sanchis-Gual¹¹⁸, V. Sandberg¹⁴³, J. R. Sanders¹⁴⁰, K. A. Santiago¹³³, N. Sarin¹⁰⁴, B. Sassolas¹²⁰, P. R. Saulson¹⁴⁰, O. Sauter²²³, R. L. Savage¹⁴³, P. Schale¹⁶⁸, M. Scheel¹⁴⁴, J. Scheuer¹⁵⁷, F. Schiettekatte²⁶², P. Schmidt¹⁶², R. Schnabel²³⁷, R. M. S. Schofield¹⁶⁸, A. Schönbeck²³⁷, E. Schreiber^{106,107}, B. W. Schulte^{106,107}, B. F. Schutz¹⁶⁶, S. G. Schwalbe¹³², J. Scott¹⁴², S. M. Scott¹¹⁹, E. Seidel¹¹⁵, D. Sellers¹⁰⁵, A. S. Sengupta²⁶³, N. Sennett¹³⁴, D. Sentenac¹²⁶, V. Sequino^{112,128,129}, A. Sergeev²³², Y. Setyawati^{106,107}, D. A. Shaddock¹¹⁹, T. Shaffer¹⁴³, M. S. Shahriar¹⁵⁷, M. B. Shaner²⁰⁸, L. Shao¹³⁴, P. Sharma¹⁵⁹, P. Shawhan¹⁷⁴, H. Shen¹¹⁵, R. Shink²⁶², D. H. Shoemaker¹¹⁰, D. M. Shoemaker¹⁷⁵, S. ShyamSundar¹⁵⁹, K. Siellez¹⁷⁵, M. Sieniawska¹⁵², D. Sigg¹⁴³, A. D. Silva¹¹¹, L. P. Singer¹⁷⁸, N. Singh¹⁷², A. Singhal^{112,130}, A. M. Sintès¹⁹⁷, S. Sitmukhambetov²⁰³, V. Skliris¹⁶⁶, B. J. J. Slagmolen¹¹⁹, T. J. Slaven-Blair¹⁶¹, J. R. Smith¹²⁴, R. J. E. Smith¹⁰⁴, S. Somala²⁶⁴, E. J. Son²³⁵, B. Sorazu¹⁴², F. Sorrentino¹⁵⁸, T. Souradeep¹⁰¹, E. Sowell¹⁸¹, A. P. Spencer¹⁴², A. K. Srivastava²⁰⁵, V. Srivastava¹⁴⁰, K. Staats¹⁵⁷, C. Stachie¹⁶³, M. Standke^{106,107}, D. A. Steer¹²⁵, M. Steinke^{106,107}, J. Steinlechner^{142,237}, S. Steinlechner²³⁷, D. Steinmeyer^{106,107}, S. P. Stevenson²⁴⁹, D. Stocks¹⁴⁷, R. Stone²⁰³, D. J. Stops¹⁰⁹, K. A. Strain¹⁴², G. Stratta^{170,171}, S. E. Strigin¹⁶⁰, A. Strunk¹⁴³, R. Sturani²⁶⁵, A. L. Stuver²⁶⁶, V. Sudhir¹¹⁰, T. Z. Summerscales²⁶⁷, L. Sun⁹⁹, S. Sunil²⁰⁵, J. Suresh¹⁰¹, P. J. Sutton¹⁶⁶, B. L. Swinkels¹³⁵, M. J. Szczepańczyk¹³², M. Tacca¹³⁵, S. C. Tait¹⁴², C. Talbot¹⁰⁴, D. Talukder¹⁶⁸, D. B. Tanner¹⁴⁶, M. Tápai²²⁰, A. Taracchini¹³⁴, J. D. Tasson¹⁹¹, R. Taylor⁹⁹, F. Thies^{106,107}, M. Thomas¹⁰⁵, P. Thomas¹⁴³, S. R. Thondapu¹⁵⁹, K. A. Thorne¹⁰⁵, E. Thrane¹⁰⁴, Shubhanshu Tiwari^{193,209}, Srishti Tiwari²²¹, V. Tiwari¹⁶⁶, K. Toland¹⁴², M. Tonelli^{116,117}, Z. Tornasi¹⁴², A. Torres-Forné²⁶⁸, C. I. Torrie⁹⁹, D. Töyrä¹⁰⁹, F. Travasso^{126,139}, G. Traylor¹⁰⁵, M. C. Tringali¹⁷², A. Trovato¹²⁵, L. Trozzo^{117,269}, R. Trudeau⁹⁹, K. W. Tsang¹³⁵, M. Tse¹¹⁰, R. Tso¹⁴⁴, L. Tsukada¹⁷⁹, D. Tsuna¹⁷⁹, D. Tuyenbayev²⁰³, K. Ueno¹⁷⁹, D. Ugolini²⁷⁰, C. S. Unnikrishnan²²¹, A. L. Urban¹⁰⁰, S. A. Usman¹⁶⁶, H. Vahlbruch¹⁰⁷, G. Vajente⁹⁹, G. Valdes¹⁰⁰, N. van Bakel¹³⁵, M. van Beuzekom¹³⁵, J. F. J. van den Brand^{135,173}, C. Van Den Broeck^{135,271}, D. C. Vander-Hyde¹⁴⁰, L. van der Schaaf¹³⁵, J. V. van Heijningen¹³⁵, A. A. van Veggel¹⁴², M. Vardaro^{149,150}, V. Varma¹⁴⁴, S. Vass⁹⁹, M. Vasúth¹⁴⁵, A. Vecchio¹⁰⁹, G. Vedovato¹⁵⁰, J. Veitch¹⁴², P. J. Veitch¹⁵³, K. Venkateswara²⁶⁰, G. Venugopalan⁹⁹, D. Verkindt¹³¹, F. Vetranò^{170,171}, A. Viceré^{170,171}, A. D. Viets¹²¹, D. J. Vine²⁶¹, J.-Y. Vinet¹⁶³, S. Vitale¹¹⁰, T. Vo¹⁴⁰, H. Vocca^{138,139}, C. Vorvick¹⁴³, S. P. Vyatchanin¹⁶⁰, A. R. Wade⁹⁹, L. E. Wade²¹², M. Wade²¹², R. Walet¹³⁵, M. Walker¹²⁴, L. Wallace⁹⁹, S. Walsh¹²¹, G. Wang^{112,117}, H. Wang¹⁰⁹, J. Z. Wang²²³, W. H. Wang²⁰³, Y. F. Wang¹⁸⁸, R. L. Ward¹¹⁹, Z. A. Warden¹³², J. Warner¹⁴³, M. Was¹³¹, J. Watchi¹⁹⁸, B. Weaver¹⁴³, L.-W. Wei^{106,107}, M. Weinert^{106,107}, A. J. Weinstein⁹⁹, R. Weiss¹¹⁰, F. Wellmann^{106,107}, L. Wen¹⁶¹, E. K. Wessel¹¹⁵, P. Weßels^{106,107}, J. W. Westhouse¹³², K. Wette¹¹⁹, J. T. Whelan¹⁵⁶, B. F. Whiting¹⁴⁶, C. Whittle¹¹⁰, D. M. Wilken^{106,107}, D. Williams¹⁴², A. R. Williamson^{135,225}, J. L. Willis⁹⁹, B. Willke^{106,107}, M. H. Wimmer^{106,107}, W. Winkler^{106,107}, C. C. Wipf⁹⁹, H. Wittel^{106,107}, G. Woan¹⁴², J. Woehler^{106,107}, J. K. Wofford¹⁵⁶, J. Worden¹⁴³, J. L. Wright¹⁴², D. S. Wu^{106,107}, D. M. Wysocki¹⁵⁶, L. Xiao⁹⁹, H. Yamamoto⁹⁹, C. C. Yancey¹⁷⁴, L. Yang²¹¹, M. J. Yap¹¹⁹, M. Yazback¹⁴⁶, D. W. Yeeles¹⁶⁶, Hang Yu¹¹⁰, Haocun Yu¹¹⁰, S. H. R. Yuen¹⁸⁸, M. Yvert¹³¹, A. K. Zadrożny²⁰³, A. Zadrożny²³⁹, M. Zanolin¹³², T. Zelenova¹²⁶, J.-P. Zendri¹⁵⁰, M. Zevin¹⁵⁷, J. Zhang¹⁶¹, L. Zhang⁹⁹, T. Zhang¹⁴², C. Zhao¹⁶¹, M. Zhou¹⁵⁷, Z. Zhou¹⁵⁷, X. J. Zhu¹⁰⁴, M. E. Zucker^{99,110}, and J. Zweizig⁹⁹

(The LIGO Scientific Collaboration and the Virgo Collaboration)

¹ Université de Strasbourg, CNRS, IPHC UMR 7178, F-67000 Strasbourg, France

² Technical University of Catalonia, Laboratory of Applied Bioacoustics, Rambla Exposició, E-08800 Vilanova i la Geltrú, Barcelona, Spain

³ INFN, Sezione di Genova, Via Dodecaneso 33, I-16146 Genova, Italy

⁴ Institut d'Investigació per a la Gestió Integrada de les Zones Costaneres (IGIC)—Universitat Politècnica de València. C/Paranímf 1, E-46730 Gandia, Spain

⁵ Aix Marseille Univ, CNRS/IN2P3, CPPM, Marseille, France

⁶ APC, Univ Paris Diderot, CNRS/IN2P3, CEA/Irfu, Obs de Paris, Sorbonne Paris Cité, France

⁷ IFIC, Instituto de Física Corpuscular (CSIC - Universitat de València) c/Catedrático José Beltrán, 2 E-46980 Paterna, Valencia, Spain
antares.spokesperson@in2p3.fr

⁸ LAM, Laboratoire d'Astrophysique de Marseille, Pôle de l'Étoile Site de Château-Gombert, rue Frédéric Joliot-Curie 38, F-13388 Marseille Cedex 13, France

⁹ National Center for Energy Sciences and Nuclear Techniques, B.P.1382, R.P.10001 Rabat, Morocco

¹⁰ INFN, Laboratori Nazionali del Sud (LNS), Via S. Sofia 62, I-95123 Catania, Italy

¹¹ Nikhef, Science Park, Amsterdam, The Netherlands

¹² Huygens-Kamerlingh Onnes Laboratorium, Universiteit Leiden, The Netherlands

¹³ University Mohammed V in Rabat, Faculty of Sciences, 4 av. Ibn Battouta, B.P. 1014, R.P. 10000 Rabat, Morocco

¹⁴ Institute of Space Science, RO-077125 Bucharest, Măgurele, Romania

¹⁵ Universiteit van Amsterdam, Instituut voor Hoge-Energie Fysica, Science Park 105, 1098 XG Amsterdam, The Netherlands

¹⁶ INFN, Sezione di Roma, P.le Aldo Moro 2, I-00185 Roma, Italy

¹⁷ Dipartimento di Fisica dell'Università La Sapienza, P.le Aldo Moro 2, I-00185 Roma, Italy

¹⁸ Gran Sasso Science Institute, Viale Francesco Crispi 7, I-00167 L'Aquila, Italy

- ¹⁹ LPHEA, Faculty of Science—Semlali, Cadi Ayyad University, P.O.B. 2390, Marrakech, Morocco
- ²⁰ INFN, Sezione di Bologna, Viale Bertini-Pichat 6/2, I-40127 Bologna, Italy
- ²¹ INFN, Sezione di Bari, Via E. Orabona 4, I-70126 Bari, Italy
- ²² Department of Computer Architecture and Technology/CITIC, University of Granada, E-18071 Granada, Spain
- ²³ Géoazur, UCA, CNRS, IRD, Observatoire de la Côte d'Azur, Sophia Antipolis, France
- ²⁴ Dipartimento di Fisica dell'Università, Via Dodecaneso 33, I-16146 Genova, Italy
- ²⁵ Université Paris-Sud, F-91405 Orsay Cedex, France
- ²⁶ Friedrich-Alexander-Universität Erlangen-Nürnberg, Erlangen Centre for Astroparticle Physics, Erwin-Rommel-Str. 1, D-91058 Erlangen, Germany
- ²⁷ University Mohammed I, Laboratory of Physics of Matter and Radiations, B.P.717, Oujda 6000, Morocco
- ²⁸ Institut für Theoretische Physik und Astrophysik, Universität Würzburg, Emil-Fischer Str. 31, D-97074 Würzburg, Germany
- ²⁹ Dipartimento di Fisica e Astronomia dell'Università, Viale Bertini Pichat 6/2, I-40127 Bologna, Italy
- ³⁰ Laboratoire de Physique Corpusculaire, Clermont Université, Université Blaise Pascal, CNRS/IN2P3, BP 10448, F-63000 Clermont-Ferrand, France
- ³¹ LIS, UMR Université de Toulon, Aix Marseille Université, CNRS, F-83041 Toulon, France
- ³² Royal Netherlands Institute for Sea Research (NIOZ) and Utrecht University, Landsdiep 4, 1797 SZ 't Horntje (Texel), The Netherlands
- ³³ Institut Universitaire de France, F-75005 Paris, France
- ³⁴ Dr. Reijers-Sternwarte and ECAP, Friedrich-Alexander-Universität Erlangen-Nürnberg, Sternwartstr. 7, D-96049 Bamberg, Germany
- ³⁵ Moscow State University, Skobel'syn Institute of Nuclear Physics, Leninskie gory, 119991 Moscow, Russia
- ³⁶ Mediterranean Institute of Oceanography (MIO), Aix-Marseille University, F-13288, Marseille, Cedex 9, France
- ³⁷ Université du Sud Toulon-Var, CNRS-INSU/IRD UM 110, F-83957, La Garde Cedex, France
- ³⁸ INFN, Sezione di Catania, Via S. Sofia 64, I-95123 Catania, Italy
- ³⁹ IRFU, CEA, Université Paris-Saclay, F-91191 Gif-sur-Yvette, France
- ⁴⁰ INFN, Sezione di Pisa, Largo B. Pontecorvo 3, I-56127 Pisa, Italy
- ⁴¹ Dipartimento di Fisica dell'Università, Largo B. Pontecorvo 3, I-56127 Pisa, Italy
- ⁴² INFN, Sezione di Napoli, Via Cintia I-80126 Napoli, Italy
- ⁴³ Dipartimento di Fisica dell'Università Federico II di Napoli, Via Cintia I-80126, Napoli, Italy
- ⁴⁴ Dpto. de Física Teórica y del Cosmos & C.A.F.P.E., University of Granada, E-18071 Granada, Spain
- ⁴⁵ GRPHE, Université de Haute Alsace—Institut universitaire de technologie de Colmar, 34 rue du Grillenbreit BP 50568-68008 Colmar, France
- ⁴⁶ Dept. of Physics and Astronomy, University of Canterbury, Private Bag 4800, Christchurch, New Zealand
- ⁴⁷ DESY, D-15738 Zeuthen, Germany
- ⁴⁸ Université Libre de Bruxelles, Science Faculty CP230, B-1050 Brussels, Belgium
- ⁴⁹ Niels Bohr Institute, University of Copenhagen, DK-2100 Copenhagen, Denmark
- ⁵⁰ Oskar Klein Centre and Dept. of Physics, Stockholm University, SE-10691 Stockholm, Sweden
- ⁵¹ Erlangen Centre for Astroparticle Physics, Friedrich-Alexander-Universität Erlangen-Nürnberg, D-91058 Erlangen, Germany
- ⁵² Department of Physics, Marquette University, Milwaukee, WI 53201, USA
- ⁵³ Dept. of Physics, Pennsylvania State University, University Park, PA 16802, USA
- ⁵⁴ Dept. of Physics, Massachusetts Institute of Technology, Cambridge, MA 02139, USA
- ⁵⁵ III. Physikalisches Institut, RWTH Aachen University, D-52056 Aachen, Germany
- ⁵⁶ Physics Department, South Dakota School of Mines and Technology, Rapid City, SD 57701, USA
- ⁵⁷ Département de physique nucléaire et corpusculaire, Université de Genève, CH-1211 Genève, Switzerland
- ⁵⁸ Dept. of Physics, University of Alberta, Edmonton, Alberta, T6G 2E1, Canada
- ⁵⁹ Dept. of Physics and Astronomy, University of California, Irvine, CA 92697, USA
- ⁶⁰ Institute of Physics, University of Mainz, Staudinger Weg 7, D-55099 Mainz, Germany
- ⁶¹ Dept. of Physics, University of California, Berkeley, CA 94720, USA
- ⁶² Dept. of Physics and Center for Cosmology and Astro-Particle Physics, Ohio State University, Columbus, OH 43210, USA
- ⁶³ Dept. of Astronomy, Ohio State University, Columbus, OH 43210, USA
- ⁶⁴ Fakultät für Physik & Astronomie, Ruhr-Universität Bochum, D-44780 Bochum, Germany
- ⁶⁵ Dept. of Physics, University of Wuppertal, D-42119 Wuppertal, Germany
- ⁶⁶ Dept. of Physics and Astronomy, University of Rochester, Rochester, NY 14627, USA
- ⁶⁷ Dept. of Physics, University of Maryland, College Park, MD 20742, USA
- ⁶⁸ Dept. of Physics and Astronomy, University of Kansas, Lawrence, KS 66045, USA
- ⁶⁹ Lawrence Berkeley National Laboratory, Berkeley, CA 94720, USA
- ⁷⁰ Dept. of Physics, TU Dortmund University, D-44221 Dortmund, Germany
- ⁷¹ Dept. of Physics and Astronomy, Uppsala University, Box 516, SE-75120 Uppsala, Sweden
- ⁷² Dept. of Physics and Wisconsin IceCube Particle Astrophysics Center, University of Wisconsin, Madison, WI 53706, USA; analysis@icecube.wisc.edu
- ⁷³ SNOLAB, 1039 Regional Road 24, Creighton Mine 9, Lively, ON, P3Y 1N2, Canada
- ⁷⁴ Institut für Kernphysik, Westfälische Wilhelms-Universität Münster, D-48149 Münster, Germany
- ⁷⁵ Vrije Universiteit Brussel (VUB), Dienst ELEM, B-1050 Brussels, Belgium
- ⁷⁶ Dept. of Astronomy and Astrophysics, Pennsylvania State University, University Park, PA 16802, USA
- ⁷⁷ School of Physics and Center for Relativistic Astrophysics, Georgia Institute of Technology, Atlanta, GA 30332, USA
- ⁷⁸ Dept. of Physics and Astronomy, Michigan State University, East Lansing, MI 48824, USA
- ⁷⁹ Bartol Research Institute and Dept. of Physics and Astronomy, University of Delaware, Newark, DE 19716, USA
- ⁸⁰ Dept. of Physics and Astronomy, University of Gent, B-9000 Gent, Belgium
- ⁸¹ Institut für Physik, Humboldt-Universität zu Berlin, D-12489 Berlin, Germany
- ⁸² Dept. of Physics, Sungkyunkwan University, Suwon 440-746, Republic of Korea
- ⁸³ Dept. of Physics, Southern University, Baton Rouge, LA 70813, USA
- ⁸⁴ Dept. of Astronomy, University of Wisconsin, Madison, WI 53706, USA
- ⁸⁵ Physik-department, Technische Universität München, D-85748 Garching, Germany
- ⁸⁶ Department of Physics, University of Adelaide, Adelaide, 5005, Australia
- ⁸⁷ Earthquake Research Institute, University of Tokyo, Bunkyo, Tokyo 113-0032, Japan
- ⁸⁸ Dept. of Physics and Institute for Global Prominent Research, Chiba University, Chiba 263-8522, Japan
- ⁸⁹ CTSPS, Clark-Atlanta University, Atlanta, GA 30314, USA
- ⁹⁰ Dept. of Physics, University of Texas at Arlington, 502 Yates St., Science Hall Rm 108, Box 19059, Arlington, TX 76019, USA
- ⁹¹ Dept. of Physics and Astronomy, Stony Brook University, Stony Brook, NY 11794-3800, USA
- ⁹² Dept. of Physics and Astronomy, University of Alabama, Tuscaloosa, AL 35487, USA
- ⁹³ Dept. of Physics, Drexel University, 3141 Chestnut Street, Philadelphia, PA 19104, USA
- ⁹⁴ Dept. of Physics, University of Wisconsin, River Falls, WI 54022, USA

- ⁹⁵ Dept. of Physics, Yale University, New Haven, CT 06520, USA
- ⁹⁶ Dept. of Physics and Astronomy, University of Alaska Anchorage, 3211 Providence Dr., Anchorage, AK 99508, USA
- ⁹⁷ Dept. of Physics, University of Oxford, 1 Keble Road, Oxford OX1 3NP, UK
- ⁹⁸ Department of Physics and Astronomy, UCLA, Los Angeles, CA 90095, USA
- ⁹⁹ LIGO, California Institute of Technology, Pasadena, CA 91125, USA; lsc-spokesperson@ligo.org, virgo-spokesperson@ego-gw.it
- ¹⁰⁰ Louisiana State University, Baton Rouge, LA 70803, USA
- ¹⁰¹ Inter-University Centre for Astronomy and Astrophysics, Pune 411007, India
- ¹⁰² Università di Salerno, Fisciano, I-84084 Salerno, Italy
- ¹⁰³ INFN, Sezione di Napoli, Complesso Universitario di Monte S. Angelo, I-80126 Napoli, Italy
- ¹⁰⁴ OzGrav, School of Physics & Astronomy, Monash University, Clayton 3800, Victoria, Australia
- ¹⁰⁵ LIGO Livingston Observatory, Livingston, LA 70754, USA
- ¹⁰⁶ Max Planck Institute for Gravitational Physics (Albert Einstein Institute), D-30167 Hannover, Germany
- ¹⁰⁷ Leibniz Universität Hannover, D-30167 Hannover, Germany
- ¹⁰⁸ University of Cambridge, Cambridge CB2 1TN, UK
- ¹⁰⁹ University of Birmingham, Birmingham B15 2TT, UK
- ¹¹⁰ LIGO, Massachusetts Institute of Technology, Cambridge, MA 02139, USA
- ¹¹¹ Instituto Nacional de Pesquisas Espaciais, 12227-010 São José dos Campos, São Paulo, Brazil
- ¹¹² Gran Sasso Science Institute (GSSI), I-67100 L'Aquila, Italy
- ¹¹³ INFN, Laboratori Nazionali del Gran Sasso, I-67100 Assergi, Italy
- ¹¹⁴ International Centre for Theoretical Sciences, Tata Institute of Fundamental Research, Bengaluru 560089, India
- ¹¹⁵ NCSA, University of Illinois at Urbana-Champaign, Urbana, IL 61801, USA
- ¹¹⁶ Università di Pisa, I-56127 Pisa, Italy
- ¹¹⁷ INFN, Sezione di Pisa, I-56127 Pisa, Italy
- ¹¹⁸ Departament de Astronomia y Astrofísica, Universitat de València, E-46100 Burjassot, València, Spain
- ¹¹⁹ OzGrav, Australian National University, Canberra, Australian Capital Territory 0200, Australia
- ¹²⁰ Laboratoire des Matériaux Avancés (LMA), CNRS/IN2P3, F-69622 Villeurbanne, France
- ¹²¹ University of Wisconsin-Milwaukee, Milwaukee, WI 53201, USA
- ¹²² SUPA, University of Strathclyde, Glasgow G1 1XQ, UK
- ¹²³ LAL, Univ. Paris-Sud, CNRS/IN2P3, Université Paris-Saclay, F-91898 Orsay, France
- ¹²⁴ California State University Fullerton, Fullerton, CA 92831, USA
- ¹²⁵ APC, AstroParticule et Cosmologie, Université Paris Diderot, CNRS/IN2P3, CEA/Irfu, Observatoire de Paris, Sorbonne Paris Cité, F-75205 Paris Cedex 13, France
- ¹²⁶ European Gravitational Observatory (EGO), I-56021 Cascina, Pisa, Italy
- ¹²⁷ Chennai Mathematical Institute, Chennai 603103, India
- ¹²⁸ Università di Roma Tor Vergata, I-00133 Roma, Italy
- ¹²⁹ INFN, Sezione di Roma Tor Vergata, I-00133 Roma, Italy
- ¹³⁰ INFN, Sezione di Roma, I-00185 Roma, Italy
- ¹³¹ Laboratoire d'Annecy de Physique des Particules (LAPP), Univ. Grenoble Alpes, Université Savoie Mont Blanc, CNRS/IN2P3, F-74941 Annecy, France
- ¹³² Embry-Riddle Aeronautical University, Prescott, AZ 86301, USA
- ¹³³ Montclair State University, Montclair, NJ 07043, USA
- ¹³⁴ Max Planck Institute for Gravitational Physics (Albert Einstein Institute), D-14476 Potsdam-Golm, Germany
- ¹³⁵ Nikhef, Science Park 105, 1098 XG Amsterdam, The Netherlands
- ¹³⁶ Korea Institute of Science and Technology Information, Daejeon 34141, Republic of Korea
- ¹³⁷ West Virginia University, Morgantown, WV 26506, USA
- ¹³⁸ Università di Perugia, I-06123 Perugia, Italy
- ¹³⁹ INFN, Sezione di Perugia, I-06123 Perugia, Italy
- ¹⁴⁰ Syracuse University, Syracuse, NY 13244, USA
- ¹⁴¹ University of Minnesota, Minneapolis, MN 55455, USA
- ¹⁴² SUPA, University of Glasgow, Glasgow G12 8QQ, UK
- ¹⁴³ LIGO Hanford Observatory, Richland, WA 99352, USA
- ¹⁴⁴ Caltech CaRT, Pasadena, CA 91125, USA
- ¹⁴⁵ Wigner RCP, RMKI, H-1121 Budapest, Konkoly Thege Miklós út 29-33, Hungary
- ¹⁴⁶ University of Florida, Gainesville, FL 32611, USA
- ¹⁴⁷ Stanford University, Stanford, CA 94305, USA
- ¹⁴⁸ Università di Camerino, Dipartimento di Fisica, I-62032 Camerino, Italy
- ¹⁴⁹ Università di Padova, Dipartimento di Fisica e Astronomia, I-35131 Padova, Italy
- ¹⁵⁰ INFN, Sezione di Padova, I-35131 Padova, Italy
- ¹⁵¹ MTA-ELTE Astrophysics Research Group, Institute of Physics, Eötvös University, Budapest 1117, Hungary
- ¹⁵² Nicolaus Copernicus Astronomical Center, Polish Academy of Sciences, 00-716, Warsaw, Poland
- ¹⁵³ OzGrav, University of Adelaide, Adelaide, South Australia 5005, Australia
- ¹⁵⁴ Theoretisch-Physikalisches Institut, Friedrich-Schiller-Universität Jena, D-07743 Jena, Germany
- ¹⁵⁵ INFN, Sezione di Milano Bicocca, Gruppo Collegato di Parma, I-43124 Parma, Italy
- ¹⁵⁶ Rochester Institute of Technology, Rochester, NY 14623, USA
- ¹⁵⁷ Center for Interdisciplinary Exploration & Research in Astrophysics (CIERA), Northwestern University, Evanston, IL 60208, USA
- ¹⁵⁸ INFN, Sezione di Genova, I-16146 Genova, Italy
- ¹⁵⁹ RRCAT, Indore, Madhya Pradesh 452013, India
- ¹⁶⁰ Faculty of Physics, Lomonosov Moscow State University, Moscow 119991, Russia
- ¹⁶¹ OzGrav, University of Western Australia, Crawley, Western Australia 6009, Australia
- ¹⁶² Department of Astrophysics/IMAPP, Radboud University Nijmegen, P.O. Box 9010, 6500 GL Nijmegen, The Netherlands
- ¹⁶³ Artemis, Université Côte d'Azur, Observatoire Côte d'Azur, CNRS, CS 34229, F-06304 Nice Cedex 4, France
- ¹⁶⁴ Physik-Institut, University of Zurich, Winterthurerstrasse 190, 8057 Zurich, Switzerland
- ¹⁶⁵ Univ Rennes, CNRS, Institut FOTON—UMR6082, F-3500 Rennes, France
- ¹⁶⁶ Cardiff University, Cardiff CF24 3AA, UK
- ¹⁶⁷ Washington State University, Pullman, WA 99164, USA
- ¹⁶⁸ University of Oregon, Eugene, OR 97403, USA
- ¹⁶⁹ Laboratoire Kastler Brossel, Sorbonne Université, CNRS, ENS-Université PSL, Collège de France, F-75005 Paris, France

- ¹⁷⁰ Università degli Studi di Urbino “Carlo Bo,” I-61029 Urbino, Italy
- ¹⁷¹ INFN, Sezione di Firenze, I-50019 Sesto Fiorentino, Firenze, Italy
- ¹⁷² Astronomical Observatory Warsaw University, 00-478 Warsaw, Poland
- ¹⁷³ VU University Amsterdam, 1081 HV Amsterdam, The Netherlands
- ¹⁷⁴ University of Maryland, College Park, MD 20742, USA
- ¹⁷⁵ School of Physics, Georgia Institute of Technology, Atlanta, GA 30332, USA
- ¹⁷⁶ Université Claude Bernard Lyon 1, F-69622 Villeurbanne, France
- ¹⁷⁷ Università di Napoli “Federico II,” Complesso Universitario di Monte S. Angelo, I-80126 Napoli, Italy
- ¹⁷⁸ NASA Goddard Space Flight Center, Greenbelt, MD 20771, USA
- ¹⁷⁹ RESCEU, University of Tokyo, Tokyo, 113-0033, Japan
- ¹⁸⁰ Tsinghua University, Beijing 100084, People’s Republic of China
- ¹⁸¹ Texas Tech University, Lubbock, TX 79409, USA
- ¹⁸² The University of Mississippi, University, MS 38677, USA
- ¹⁸³ Museo Storico della Fisica e Centro Studi e Ricerche “Enrico Fermi,” I-00184 Roma, Italy
- ¹⁸⁴ The Pennsylvania State University, University Park, PA 16802, USA
- ¹⁸⁵ National Tsing Hua University, Hsinchu City, 30013 Taiwan, Republic of China
- ¹⁸⁶ Charles Sturt University, Wagga Wagga, New South Wales 2678, Australia
- ¹⁸⁷ University of Chicago, Chicago, IL 60637, USA
- ¹⁸⁸ The Chinese University of Hong Kong, Shatin, NT, Hong Kong
- ¹⁸⁹ Seoul National University, Seoul 08826, Republic of Korea
- ¹⁹⁰ Pusan National University, Busan 46241, Republic of Korea
- ¹⁹¹ Carleton College, Northfield, MN 55057, USA
- ¹⁹² INAF, Osservatorio Astronomico di Padova, I-35122 Padova, Italy
- ¹⁹³ INFN, Trento Institute for Fundamental Physics and Applications, I-38123 Povo, Trento, Italy
- ¹⁹⁴ Dipartimento di Fisica, Università degli Studi di Genova, I-16146 Genova, Italy
- ¹⁹⁵ OzGrav, University of Melbourne, Parkville, Victoria 3010, Australia
- ¹⁹⁶ Columbia University, New York, NY 10027, USA
- ¹⁹⁷ Universitat de les Illes Balears, IAC3—IEEC, E-07122 Palma de Mallorca, Spain
- ¹⁹⁸ Université Libre de Bruxelles, Brussels B-1050, Belgium
- ¹⁹⁹ Sonoma State University, Rohnert Park, CA 94928, USA
- ²⁰⁰ Departamento de Matemáticas, Universitat de València, E-46100 Burjassot, València, Spain
- ²⁰¹ Montana State University, Bozeman, MT 59717, USA
- ²⁰² University of Rhode Island, Kingston, RI 02881, USA
- ²⁰³ The University of Texas Rio Grande Valley, Brownsville, TX 78520, USA
- ²⁰⁴ Bellevue College, Bellevue, WA 98007, USA
- ²⁰⁵ Institute for Plasma Research, Bhat, Gandhinagar 382428, India
- ²⁰⁶ The University of Sheffield, Sheffield S10 2TN, UK
- ²⁰⁷ Dipartimento di Scienze Matematiche, Fisiche e Informatiche, Università di Parma, I-43124 Parma, Italy
- ²⁰⁸ California State University, Los Angeles, 5151 State University Dr, Los Angeles, CA 90032, USA
- ²⁰⁹ Università di Trento, Dipartimento di Fisica, I-38123 Povo, Trento, Italy
- ²¹⁰ Università di Roma “La Sapienza,” I-00185 Roma, Italy
- ²¹¹ Colorado State University, Fort Collins, CO 80523, USA
- ²¹² Kenyon College, Gambier, OH 43022, USA
- ²¹³ Christopher Newport University, Newport News, VA 23606, USA
- ²¹⁴ National Astronomical Observatory of Japan, 2-21-1 Osawa, Mitaka, Tokyo 181-8588, Japan
- ²¹⁵ Canadian Institute for Theoretical Astrophysics, University of Toronto, Toronto, Ontario M5S 3H8, Canada
- ²¹⁶ Observatori Astronòmic, Universitat de València, E-46980 Paterna, València, Spain
- ²¹⁷ School of Mathematics, University of Edinburgh, Edinburgh EH9 3FD, UK
- ²¹⁸ Institute Of Advanced Research, Gandhinagar 382426, India
- ²¹⁹ Indian Institute of Technology Bombay, Powai, Mumbai 400 076, India
- ²²⁰ University of Szeged, Dóm tér 9, Szeged 6720, Hungary
- ²²¹ Tata Institute of Fundamental Research, Mumbai 400005, India
- ²²² INAF, Osservatorio Astronomico di Capodimonte, I-80131, Napoli, Italy
- ²²³ University of Michigan, Ann Arbor, MI 48109, USA
- ²²⁴ American University, Washington, D.C. 20016, USA
- ²²⁵ GRAPPA, Anton Pannekoek Institute for Astronomy and Institute of High-Energy Physics, University of Amsterdam, Science Park 904, 1098 XH Amsterdam, The Netherlands
- ²²⁶ Delta Institute for Theoretical Physics, Science Park 904, 1090 GL Amsterdam, The Netherlands
- ²²⁷ Directorate of Construction, Services & Estate Management, Mumbai 400094 India
- ²²⁸ University of Białystok, 15-424 Białystok, Poland
- ²²⁹ King’s College London, University of London, London WC2R 2LS, UK
- ²³⁰ University of Southampton, Southampton SO17 1BJ, UK
- ²³¹ University of Washington Bothell, Bothell, WA 98011, USA
- ²³² Institute of Applied Physics, Nizhny Novgorod, 603950, Russia
- ²³³ Ewha Womans University, Seoul 03760, Republic of Korea
- ²³⁴ Inje University Gimhae, South Gyeongsang 50834, Republic of Korea
- ²³⁵ National Institute for Mathematical Sciences, Daejeon 34047, Republic of Korea
- ²³⁶ Ulsan National Institute of Science and Technology, Ulsan 44919, Republic of Korea
- ²³⁷ Universität Hamburg, D-22761 Hamburg, Germany
- ²³⁸ Maastricht University, P.O. Box 616, 6200 MD Maastricht, The Netherlands
- ²³⁹ NCBJ, 05-400 Świerk-Otwock, Poland
- ²⁴⁰ Institute of Mathematics, Polish Academy of Sciences, 00656 Warsaw, Poland
- ²⁴¹ Cornell University, Ithaca, NY 14850, USA
- ²⁴² Hillsdale College, Hillsdale, MI 49242, USA
- ²⁴³ Hanyang University, Seoul 04763, Republic of Korea
- ²⁴⁴ Korea Astronomy and Space Science Institute, Daejeon 34055, Republic of Korea

- ²⁴⁵ NASA Marshall Space Flight Center, Huntsville, AL 35811, USA
²⁴⁶ Dipartimento di Matematica e Fisica, Università degli Studi Roma Tre, I-00146 Roma, Italy
²⁴⁷ INFN, Sezione di Roma Tre, I-00146 Roma, Italy
²⁴⁸ ESPCI, CNRS, F-75005 Paris, France
²⁴⁹ OzGrav, Swinburne University of Technology, Hawthorn VIC 3122, Australia
²⁵⁰ University of Portsmouth, Portsmouth, PO1 3FX, UK
²⁵¹ Southern University and A&M College, Baton Rouge, LA 70813, USA
²⁵² College of William and Mary, Williamsburg, VA 23187, USA
²⁵³ Centre Scientifique de Monaco, 8 quai Antoine 1er, MC-98000, Monaco
²⁵⁴ Indian Institute of Technology Madras, Chennai 600036, India
²⁵⁵ IISER-Kolkata, Mohanpur, West Bengal 741252, India
²⁵⁶ Whitman College, 345 Boyer Avenue, Walla Walla, WA 99362 USA
²⁵⁷ Université de Lyon, F-69361 Lyon, France
²⁵⁸ Hobart and William Smith Colleges, Geneva, NY 14456, USA
²⁵⁹ Janusz Gil Institute of Astronomy, University of Zielona Góra, 65-265 Zielona Góra, Poland
²⁶⁰ University of Washington, Seattle, WA 98195, USA
²⁶¹ SUPA, University of the West of Scotland, Paisley PA1 2BE, UK
²⁶² Université de Montréal/Polytechnique, Montreal, Quebec H3T 1J4, Canada
²⁶³ Indian Institute of Technology, Gandhinagar Ahmedabad Gujarat 382424, India
²⁶⁴ Indian Institute of Technology Hyderabad, Sangareddy, Khandi, Telangana 502285, India
²⁶⁵ International Institute of Physics, Universidade Federal do Rio Grande do Norte, Natal RN 59078-970, Brazil
²⁶⁶ Villanova University, 800 Lancaster Ave, Villanova, PA 19085, USA
²⁶⁷ Andrews University, Berrien Springs, MI 49104, USA
²⁶⁸ Max Planck Institute for Gravitationalphysik (Albert Einstein Institute), D-14476 Potsdam-Golm, Germany
²⁶⁹ Università di Siena, I-53100 Siena, Italy
²⁷⁰ Trinity University, San Antonio, TX 78212, USA
²⁷¹ Van Swinderen Institute for Particle Physics and Gravity, University of Groningen, Nijenborgh 4, 9747 AG Groningen, The Netherlands
 Received 2018 October 24; revised 2018 November 14; accepted 2018 November 16; published 2019 January 16

Abstract

Astrophysical sources of gravitational waves, such as binary neutron star and black hole mergers or core-collapse supernovae, can drive relativistic outflows, giving rise to non-thermal high-energy emission. High-energy neutrinos are signatures of such outflows. The detection of gravitational waves and high-energy neutrinos from common sources could help establish the connection between the dynamics of the progenitor and the properties of the outflow. We searched for associated emission of gravitational waves and high-energy neutrinos from astrophysical transients with minimal assumptions using data from Advanced LIGO from its first observing run O1, and data from the ANTARES and IceCube neutrino observatories from the same time period. We focused on candidate events whose astrophysical origins could not be determined from a single messenger. We found no significant coincident candidate, which we used to constrain the rate density of astrophysical sources dependent on their gravitational-wave and neutrino emission processes.

Key words: gravitational waves – neutrinos

1. Introduction

We have entered the era of regular gravitational-wave (GW) discoveries. Since 2015, Advanced LIGO (Abadie et al. 2015) and Advanced Virgo (Acernese et al. 2015) have discovered GWs from multiple binary black hole mergers (Abbott et al. 2016a, 2017a, 2017b, 2017c) and a binary neutron star (BNS) merger (Abbott et al. 2017d, 2018a) during Advanced LIGO’s first two and Advanced Virgo’s first observing periods. The rate of detections is expected to significantly increase in upcoming observation periods (Abbott et al. 2018b).

High-energy neutrinos carry information about hadronic acceleration in astrophysical phenomena, such as accreting black holes and supernovae (Halzen & Hooper 2002) and about the environment of the emission site (e.g., Razzaque et al. 2003; Loeb & Waxman 2006; Bartos et al. 2012). Several high-energy

neutrino observatories carry out joint searches with GW and electromagnetic facilities. The primary facilities are the IceCube Neutrino Observatory (hereafter IceCube), a gigaton Cherenkov detector located in the ice at the South Pole (Aartsen et al. 2017a); the ANTARES neutrino telescope (hereafter ANTARES), a 10 megaton-scale underwater Cherenkov detector in the Mediterranean Sea (Ageron et al. 2011); and the Pierre Auger Cosmic Ray Observatory (Aab et al. 2015).

A quasi-diffuse high-energy neutrino flux of cosmic origin has been identified by the IceCube Neutrino Observatory (Aartsen et al. 2013a, 2013b), at a flux level consistent with the latest constraints by the ANTARES neutrino detector (Albert et al. 2018a). Evidence of neutrino emission from the blazar TXS 0506+056 provides the strongest indication to date that at least a fraction of the cosmic neutrinos are produced in blazars (Aartsen et al. 2018; Albert et al. 2018b).

Neutrinos detected via charged-current ν_μ interactions can be reconstructed with an angular uncertainty $\lesssim 1^\circ$. Since the directions of GWs can be reconstructed to within tens to hundreds of square degrees, a joint GW+neutrino observation could significantly improve the localization of a GW source, making electromagnetic follow-up observations faster and more feasible. In addition, combining the GW and neutrino

²⁷² Deceased, 2018 February.

²⁷³ Deceased, 2017 November.

²⁷⁴ Deceased, 2018 July.



data allows us to identify candidates that would not otherwise be significant for either GW or neutrino data alone.

No common sources of GWs and high-energy neutrinos have been identified so far. Until now, observational constraints for astrophysical source populations have only been derived using Initial LIGO and Virgo, and the partially completed IceCube and ANTARES detectors (Bartos et al. 2011; Adrián-Martínez et al. 2013a; Aartsen et al. 2014a). In addition, searches have been carried out for the neutrino counterparts of binary black hole mergers detected during Advanced LIGO’s first (Aab et al. 2016; Abe et al. 2016; Adrián-Martínez et al. 2016a; Gando et al. 2016; Agostini et al. 2017; Albert et al. 2017a) and second observing runs (Agostini et al. 2017; Albert et al. 2017b), and BNS merger GW170817/GRB 170817A (Albert et al. 2017c; Abe et al. 2018).

In this paper we present a multimessenger search for common transient sources of GWs and high-energy neutrinos using GW data from Advanced LIGO’s first observing run (O1) and neutrino data from both ANTARES and IceCube.

The paper is organized as follows. In Section 2, we describe the GW and neutrino observatories, and the data used in this analysis. We also briefly introduce our multimessenger search method. In Section 3, we present the results of our combined search and the corresponding constraints on astrophysical populations. We present our conclusions in Section 4.

2. Detectors and Data Analysis

2.1. Advanced LIGO

Advanced LIGO’s O1 observing run started on 2015 September 12, and lasted until 2016 January 19. During this period, Advanced LIGO had an unprecedented sensitivity to GW transients, which led to the discovery of multiple astrophysical GW signals (Abbott et al. 2016a).

We used the data from Advanced LIGO’s two detectors in Hanford, Washington and Livingston, Louisiana, to carry out a generic GW transient search, called coherent WaveBurst (cWB; Klimenko et al. 2008, 2011, 2016), using minimal assumptions on the source properties. We adopted the triggers from the all-sky, unmodeled, short duration, transient search reported by LIGO and Virgo Abbott et al. (2016b). In this, we quantified the significance of GW event candidates using a test statistic ρ constructed in the framework of constrained maximum likelihood analysis (Klimenko et al. 2008). We considered GW signal candidates with $\rho \geq 6$, corresponding to a GW false alarm rate (FAR) $\text{FAR}_{\text{GW}} \approx 1 \text{ day}^{-1}$. Beyond ρ , cWB outputs the time of the GW candidate, as well as its directional probability distribution, or *skymap* (Klimenko et al. 2011). We calculate the GW skymap either up to its 90% confidence region, or up to 320 deg^2 divided into 2000 tiles of 0.4×0.4 size, whichever is smaller.

We assign each GW candidate one of three classifications, C1, C2, or C3, based on its time-frequency morphology (Abbott et al. 2016b, 2017e). These labels are assigned to help separate likely noise transients from other events. Candidates with frequency evolutions consistent with noise fluctuations often occurring in LIGO-Virgo data were placed into class C1. Multiple time-frequency morphologies were included. An example category is events for which at least 80% of GW energy is within a bandwidth of 5 Hz. Such a narrow band is characteristic of power and mechanical resonance lines in GW detectors.

From the remaining candidates, those whose frequency increases with time, i.e., those similar in morphology to compact binary mergers, were placed in class C3. All other GW candidates were placed in class C2 (Abbott et al. 2016b, 2017e).

This grouping reduces the FAR for events within C2 and C3, without eliminating the chance of identifying a high-significance signal in C1.

In this search we used the C2 and C3 classes together, which have a higher probability of being astrophysical, and treated the C1 class separately. We calculated the background distribution of the test statistic separately for these two categories. For a given event, its GW p -value p_{GW} is calculated by comparing the reconstructed ρ value to the background distribution of ρ in the same category as the event. Because the C1 and C2+C3 searches are statistically independent, we include a trial factor of 2 in our final significance.

Overall, cWB identified 46 GW candidates during the $T_{\text{obs}} = 48.6$ days of coincident data from the LIGO Hanford and LIGO Livingston detectors, which is consistent with our background expectation. Of these candidates, 23 fell into the C1 category, while 23 were identified as C2+C3.

To characterize the background distribution of the ranking statistic ρ for GW candidates, we carried out the same search over GW data after applying time shifts between the data from the two LIGO detectors, with time shifts much greater than the travel time of GWs between the LIGO detectors (10 ms). This technique ensures that no short GW transient appears simultaneously in the data streams of the two detectors, and is therefore able to characterize the performance of the search in the detector noise. We carried out the analysis over 500 different time shifts to collect a large background data set. We found a total of 23,494 background GW candidates with $\rho \geq 6$. A subset of 11,005 of these were identified as C1, while 12,489 were C2+C3. The FARs for C1 and C2+C3 are both $\sim 0.5 \text{ day}^{-1}$.

2.2. IceCube

IceCube is a cubic-kilometer-sized neutrino observatory (Aartsen et al. 2017a) installed in the ice at the geographic South Pole in Antarctica between depths of 1450 and 2450 m. It is a gigaton-scale array of photosensors with a duty cycle higher than 99%. IceCube observes neutrinos coming from all directions, but by using the Earth as a shield to block background cosmic ray-induced muons, it achieves a very high detection efficiency for neutrinos originating in the northern celestial hemisphere with energies above $\mathcal{O}(1)\text{TeV}$. Neutrinos originating in the southern sky are detected with high efficiency above $\mathcal{O}(100)\text{TeV}$.

IceCube is sensitive to all neutrino flavors and both charged-current and neutral current interactions. For this search we focus on muon neutrinos that produce muons in charged-current interactions. These neutrinos are the most suitable for the search, due to their superior angular reconstructions and high detection efficiency in the northern sky.

We adopted a selection of through-going muons used in IceCube’s online analyses (Kintscher et al. 2016; Aartsen et al. 2017b), which follows an event selection similar to that used in point-source searches (Aartsen et al. 2017c). This event selection picks out primarily cosmic-ray-induced background events, with an expectation of 4.0 events in the northern sky (predominantly generated by atmospheric neutrinos) and

2.7 events in the southern sky (predominantly muons generated by high-energy cosmic rays interactions in the atmosphere above the detector) per 1000 s.

Between the beginning and the end of LIGO's O1 observing run, we identified 41,985 neutrino candidates using IceCube's online analysis. The analysis determined the time of arrival, reconstructed energy, as well as the directional point-spread function of each neutrino candidate.

2.3. ANTARES

The ANTARES neutrino telescope, located deep (2500 m) in the Mediterranean Sea, 40 km from Toulon, France, has been continuously operating since 2008. It is a 10 megaton-scale array of photosensors, detecting neutrinos with energies above $\mathcal{O}(100)\text{GeV}$, with a duty cycle higher than 90%.

The selection criteria for the ANTARES neutrino candidates were optimized based on the observed background rate and followed the same philosophy as the one used in the follow-up of GW170817 (Albert et al. 2017c). The events were selected from the most recent offline-reconstructed data set, that incorporated dedicated calibrations, in terms of positioning (Adrián-Martínez et al. 2012), timing (Aguilar et al. 2011), and efficiency (Aguilar et al. 2007). Only upgoing ν_μ neutrino candidates, detected by their muon tracks, were considered in this analysis.

A time-dependent selection criterion, based on the quality of the muon track reconstruction, was optimized such that a selected high-energy neutrino event in a time window of thousands and within the 90% confidence contour of a GW would yield a significance of 3σ , i.e., have a probability of less than 2.7×10^{-3} of arising due to atmospheric backgrounds. We rely on a sample of simulated GW events (Singer et al. 2014) to extract a relationship between the signal-to-noise ratio of an event and the area of the 90% confidence region for the GW localization. This latter relation is used to extrapolate the size of the confidence region to sub-threshold GW events. This size is then convolved with the ANTARES visible sky and its acceptance in local coordinates, to obtain the median 90% confidence region of possible GW events.

In this specific study, the reduced time and space windows enable us to decrease the associated background, and therefore to relax the quality criteria that classify reconstructed tracks as upward going events. As a consequence the dominant background component is downgoing atmospheric muons misreconstructed as upgoing, hence mimicking neutrino-induced muons.

Each event is characterized by its detection time, arrival direction, directional uncertainty, and number of detected photons. The latter is used here as an energy proxy.

The ANTARES trigger rate varies with the environmental conditions, in particular the ambient background, which is correlated with the sea current. Thus, using a time-dependent selection criterion instead of a constant value as used in point-source searches allows an increase in the number of selected signal events. For an E^{-2} spectrum the improvement is $45\% \pm 15\%$, depending on the time and data-taking conditions. This optimization improves the volume probed and correspondingly the number of detectable joint GW+high-energy neutrino sources by the ANTARES component of the joint analysis, by a factor 1.5–2.

With this new analysis, which considers the detector sensitivity at the time of the GW candidate, we obtain a total

of 907 selected high-energy neutrino candidates with ANTARES between the beginning and end of the O1 observation run, corresponding to an expected average of 0.1 neutrinos within a 1000 s time window.

2.4. Multimessenger Analysis

We jointly analyzed GW and neutrino event candidates to search for common sources using a multimessenger search algorithm (Baret et al. 2012), which was already followed in a previous joint search (Aartsen et al. 2014a). We used the significance of GW and neutrino candidates independently, as well as their temporal and directional coincidence, to quantify the significance of joint events.

We adopted ρ as the ranking statistic for GW candidates. We calculated the significance of GW candidate i by calculating its p -value $p_{\text{GW},i}$ based on its ρ_i value, separately for the C1 and C2+C3 classes. That is, $p_{\text{GW},i}$ is defined as the fraction of background GW candidates with $\rho \geq \rho_i$ and within the same signal category as GW candidate i . For neutrino candidates, we used their reconstructed energy ϵ_ν as the ranking statistic. For ANTARES, ϵ_ν is approximated with the number of detected photons corresponding to a given event, while for IceCube it is the energy reconstructed by the detection algorithm. We calculated the significance of neutrino candidate j by calculating its p -value $p_{\nu,j}$ based on the energy proxy $\epsilon_{\nu,j}$. In the following for simplicity we will refer to this as the reconstructed energy. For IceCube, we considered all detected neutrino candidates within a decl. band of $\pm 5^\circ$ around the decl. of candidate j . The candidate's p -value was then calculated as the fraction of background neutrino candidates within this band with energies $\epsilon_\nu \geq \epsilon_{\nu,j}$. This calculation accounts for the fact that the energy distribution for neutrino candidates in IceCube changes little with R.A., but depends strongly on decl. For ANTARES, $p_{\nu,j}$ was calculated using Monte Carlo simulations as a probability of observing a neutrino energy $\epsilon_\nu \geq \epsilon_{\nu,j}$ given the observed neutrino direction.

In this analysis, temporal coincidence is a binary classification. Any neutrino arriving within ± 500 s of a GW candidate is considered temporally coincident (Baret et al. 2011). Directional coincidence is quantified as the product of the GW skymap and neutrino reconstructed point-spread function, marginalized over the whole sky.

In order to quantify the significance of joint event candidates, we carried out a Monte Carlo simulation to obtain their background distribution. One realization consisted of the following steps. (i) We randomly select a GW event candidate from the candidates identified in time-shifted GW data. (ii) We randomly select a neutrino candidate from the set of all observed neutrino candidates, and assign this to the selected GW candidate. We keep its original parameters, other than its time of arrival, which is changed to reflect the fact that we consider the two events to be temporally coincident. Importantly, we fix the neutrino's direction with respect to the neutrino detector's position, and calculate its R.A. and decl. by assuming it arrived at the same time as the GW candidate it was assigned to.

We realized 20,000 times the steps described above both for the case of ANTARES and for IceCube, and used these background simulations to calculate the p -value p_{sky} of directional coincidence.

For neutrino candidates in temporal coincidence with GW candidates, we combined the three p -values from above into

one ranking statistic X^2 , following Fisher's method (Fisher 1925):

$$X^2 = -2 \ln(p_{\text{GW}} \cdot p_\nu \cdot p_{\text{sky}}). \quad (1)$$

For neutrino candidates not in such coincidence we assigned $X^2 = 0$. This results in a X^2 distribution with one component of positive values distributed according to the coincidence simulation described above, and one component located at zero. The fraction in the former component, i.e., the fraction of neutrino background events in GW coincidence, is $1 - \text{Poiss}(0, \text{FAR}_{\text{GW}}\Delta T)$. Here, $\text{Poiss}(k, \lambda)$ is the Poisson probability of observing k events given λ expected events, and $\Delta T = 1000$ s is our search time window.

We quantified the significance of joint signal candidate i using the p -value

$$p_{\text{GW}+\nu}^{(i)} = \int_{X_i^2}^{\infty} p_{\text{BG}}(X'^2) dX'^2, \quad (2)$$

where $p_{\text{BG}}(X^2)$ is the distribution of X^2 for background events. Note that this p -value is defined for every neutrino candidate, also those not in temporal coincidence with a GW. For the latter category $p_{\text{GW}+\nu}^{(i)}$.

A more detailed description of the method can be found in Baret et al. (2012).

2.5. Calculating Population Constraints

The expected amplitude h_{rssi} from a source depends on its distance r as well as its total radiated GW energy E_{GW} :

$$h_{\text{rssi}}(E_{\text{GW}}, r) = \frac{\kappa G^{1/2} E_{\text{GW}}^{1/2}}{\pi c^{3/2} r f_0}, \quad (3)$$

where c is the speed of light, G is the gravitational constant, f_0 is the characteristic frequency of the GW, and κ is an $\mathcal{O}(1)$ dimensionless constant, which we take to be $(5/2)^{1/2}$ (Sutton 2013). This value corresponds to a rotational GW source, such as a BNS merger or a rapidly rotating neutron star.

We model the expected high-energy neutrino spectrum as $dn_\nu/dE_\nu = \Phi_0 E_\nu^{-2}$ within the energy band $E_\nu \in [100 \text{ GeV}, 100 \text{ PeV}]$. For this model the neutrino spectral parameter Φ_0 at Earth is $\Phi_0 = E_{\nu, \text{iso}}(4\pi r^2)^{-1}/6$, where $E_{\nu, \text{iso}}$ is total isotropic-equivalent energy emitted in neutrinos. Combining Φ_0 with the detectors' effective areas we can calculate the expected number of detected neutrinos $\langle N_\nu \rangle$. This in turn determines the probability that at least one neutrino will be detected from the source, given that it is beamed toward the observer:

$$p_{\text{det}, \nu, X}(E_{\nu, \text{iso}}, r) = 1 - \text{Poiss}(0, \langle N_\nu \rangle_X). \quad (4)$$

Upon non-detection, we can obtain constraints on the population of GW+neutrino sources. Let $f_{\text{GW,IC}}(h_{\text{rssi}})$ and $f_{\text{GW,A}}(h_{\text{rssi}})$ be the fractions of GW+neutrino events with h_{rssi} root-sum-squared GW strain amplitude that are expected to surpass a specific significance, here taken as that of our most significant event. Here and below, the subscript IC is used for IceCube and A is used for ANTARES. We only consider the fraction of GW events here that have a temporally coincident neutrino candidate.

The rate upper limit R_{UL} of common sources will then be

$$R_{\text{UL}} = \frac{3.9 f_b}{T_{\text{obs}}} \left[\int_0^\infty 4\pi r^2 p_{\text{det}} dr \right]^{-1}, \quad (5)$$

where $f_b \equiv (1 - \cos \theta_j)^{-1}$ is the neutrino emission's beaming factor for jet-opening half-angle θ_j , the factor 3.9 arises from the Poisson distribution and corresponds to a Neyman 90% confidence-level upper limit, and

$$p_{\text{det}} = f_{\text{GW,IC}} \cdot p_{\text{det}, \nu, \text{IC}} + f_{\text{GW,A}} \cdot p_{\text{det}, \nu, \text{A}} - f_{\text{GW,IC}} \cdot f_{\text{GW,A}} \cdot p_{\text{det}, \nu, \text{IC}} \cdot p_{\text{det}, \nu, \text{A}}. \quad (6)$$

Here, the last term on the right side ensures that a simultaneous detection by IceCube and ANTARES is not counted twice.

3. Results

We found that 42 of the 46 GW event candidates had temporally coincident neutrino candidates for IceCube, with a total of 195 coincident neutrinos. We identified no temporally coincident neutrino candidates for ANTARES. These results are consistent with our background expectation.

None of the joint GW+neutrino candidates we identified have sufficiently high significance to consider them a detection. Our most significant event corresponds to a GW candidate recorded on 2015 December 18 at 11:40:17 UTC, and a neutrino candidate observed 296 s later. There is a strong directional coincidence between the candidates, with $p_{\text{sky}} = 0.01$. The GW p -value for the event is $p_{\text{GW}} = 10^{-3}$. The GW candidate is classified as C2+C3. The neutrino candidate was detected at (R.A., decl.) = (312°5, -25°3). It had a reconstructed muon energy of 127.3 TeV. This is a typical energy for a background event in the southern sky, and corresponds to a neutrino p -value of $p_\nu = 0.43$. The p -value of our most significant event, considering the whole observing run, is 0.82, making our results consistent with expectations from the background.

3.1. Sensitivity

We calculated the sensitivity of our search using simulated multimessenger signals. We generated gravitational waveforms with varying amplitudes that we superimposed on the data. We adopted a sine-Gaussian gravitational waveform with characteristic frequency $f_0 = 153$ Hz and quality factor $Q = 9$. This standard waveform has been used for past searches, which allows comparison to prior results and the characterization of sensitivity (see, e.g., Abadie et al. 2010). The sensitivity of GW detectors gradually decreases for frequencies away from the most sensitive band around 200 Hz. See Beauville et al. (2008) for a comparison of search sensitivities and Klimentenko et al. (2011) for a comparison for localization accuracy for different gravitational waveforms.

We used Monte Carlo simulations to generate a set of detected astrophysical high-energy neutrinos. We draw the energies of the incoming neutrinos from a distribution of $dn_\nu/dE_\nu \propto E_\nu^{-2}$, consistent with the scaling expected for particle acceleration in relativistic jets (Waxman & Bahcall 1997). A softer spectrum, or the addition of a spectral cutoff, would make our resulting sensitivity somewhat weaker (Adrián-Martínez et al. 2016a). We chose a lower limit for the neutrino energies of 300 GeV for IceCube and 100 GeV for ANTARES.

We evaluated our search sensitivity as follows. For a given GW signal amplitude and assuming an astrophysical neutrino was detected from the source, we calculate the fraction of simulated GW+neutrino events that are reconstructed with $p_{\text{GW}+\nu}$ below a threshold value. This gives us $f_{\text{GW,IC}}(h_{\text{rssi}})$ and

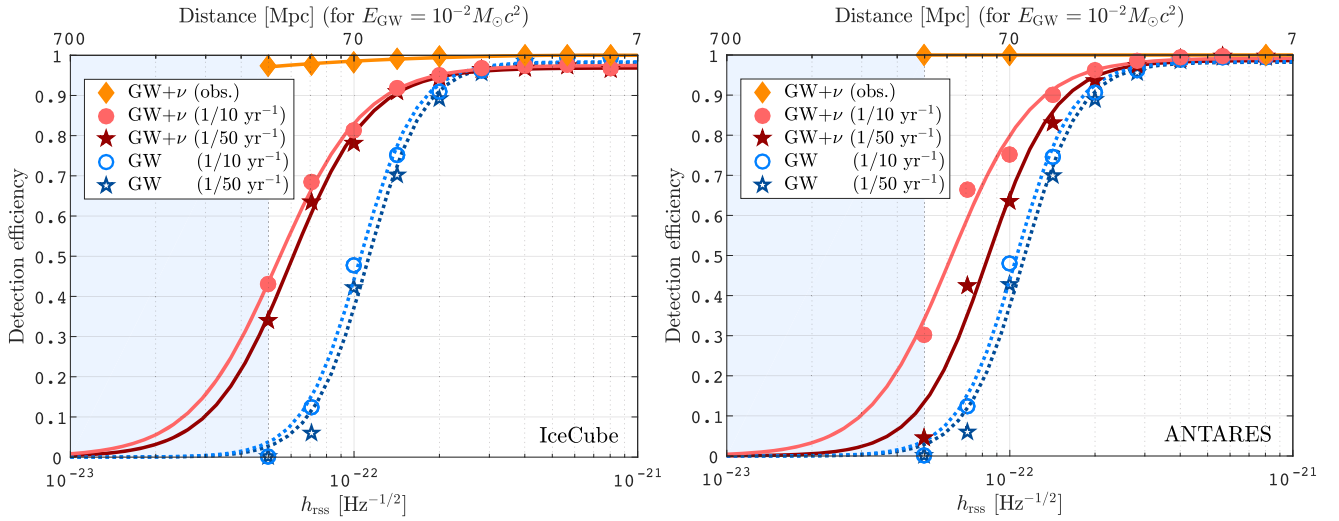


Figure 1. Fraction of simulated astrophysical GW+neutrino events whose significance exceeds a threshold as a function of the GW h_{rss} , assuming a sine-Gaussian gravitational waveform described in Section 3.1. Separate curves are shown for the cases of detections by IceCube+LIGO (left) and ANTARES+LIGO (right). Results are shown for different significance thresholds, with thresholds set at the most significant event [GW+ ν (obs.)], as well as thresholds corresponding to FARs 1/10 yr $^{-1}$ and 1/50 yr $^{-1}$. For comparison, we further show results for GW-only searches, also for FARs 1/10 yr $^{-1}$ and 1/50 yr $^{-1}$. On the top of the figures we also show the source distance corresponding to h_{rss} , assuming $E_{\text{GW}} = 10^{-2} M_{\odot} c^2$. Below 5×10^{-23} , we find that the GW search is unable to detect events (shaded area).

$f_{\text{GW,A}}(h_{\text{rss}})$, as defined earlier. We calculate these fractions for a range of GW signal amplitudes, characterized by the root-sum-squared GW strain h_{rss} . We compute fractions for multiple thresholds:

(i) First, we consider $p_{\text{GW}+\nu}$ of our most significant event for IceCube. For ANTARES, as there was no coincident GW+neutrino event, any coincidence by itself passes our threshold.

(ii) We consider the expected most significant background events over 10 and 50 yr observation periods. To obtain these thresholds, we use Monte Carlo simulations to generate multiple realizations of 10 and 50 yr joint observation periods, and for each realization we find the event with the lowest $p_{\text{GW}+\nu}$.

Figure 1 shows our search’s detection efficiency as a function of h_{rss} , separately for IceCube and ANTARES, for different significance thresholds. We also show results for both GW+neutrino and GW-only sensitivities. For example, for $h_{\text{rss}} = 10^{-22}$ Hz $^{-1/2}$ we find that 80% of those GW+neutrino injections for which a neutrino is detected will have FAR < 1/50 yr $^{-1}$, while only 43% of GW events have FAR < 1/50 yr $^{-1}$. We also find that below $h_{\text{rss}} = 5 \times 10^{-23}$ Hz $^{-1/2}$ the GW search is unable to detect these events.

We also see in Figure 1 how our sensitivity changes if instead of the most significant event of the present search we use as threshold a FAR of 1/10 yr $^{-1}$ and 1/50 yr $^{-1}$. For comparison, we also show the sensitivity curve for GW-only searches. We see that there is little difference between results for 1/10 yr $^{-1}$ and 1/50 yr $^{-1}$ FAR values, for either detector.

3.2. Population Constraints

We used our non-detection to obtain constraints on the population of GW+neutrino sources. We carried out Monte Carlo simulations to compute the direction-dependent effective area of the detectors, separately for IceCube and ANTARES. Adopting a neutrino spectrum $E_{\nu}^2 dn_{\nu} / dE_{\nu} = \Phi_0$, where n_{ν} is the neutrino fluence at the detector, we found that the sky-averaged expected number of detected neutrinos are

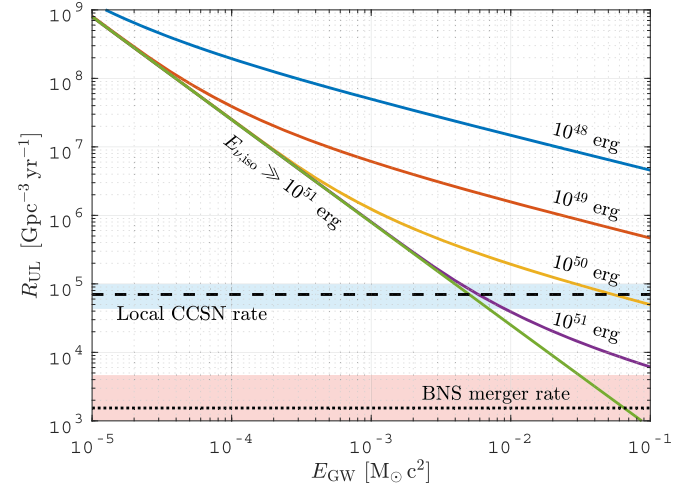


Figure 2. Upper limits for the rate density of GW+neutrino sources as functions of E_{GW} , for different values of $E_{\text{iso},\nu}$ (see numerical values of $E_{\text{iso},\nu}$ in the figure), for a sine-Gaussian gravitational waveform described in Section 3.1. We assume a beaming factor $f_b = 10$. For comparison, we show the rate density of local core-collapse supernovae (CCSN; dashed line, rate error region shown in blue), and that of BNS mergers (dotted line, rate error region shown in red).

$\langle N_{\nu} \rangle_{\text{IC}} = 30(\Phi_0/\text{GeV cm}^{-2})$ and $\langle N_{\nu} \rangle_{\text{A}} = 1.2(\Phi_0/\text{GeV cm}^{-2})$ for IceCube (IC) and ANTARES (A), respectively.

We used $f_{\text{GW,IC}}(h_{\text{rss}})$ and $f_{\text{GW,A}}(h_{\text{rss}})$ along with $\langle N_{\nu} \rangle$ to calculate p_{det} using Equation (6), which we substituted into Equation (5) to obtain the population rate upper limit R_{UL} . Figure 2 shows our results for R_{UL} for different source parameters.

In Figure 2 we assume a beaming factor of $f_b = 10$. The constraints linearly scale with f_b . The expected beaming factor varies between sources. For low-luminosity gamma-ray bursts (GRBs), it can be as low as $f_b \lesssim 14$ (Liang et al. 2007). For long GRBs, typical jet-opening angles are $\theta_j = 3^{\circ}$ – 10° , with some extending up to $\approx 20^{\circ}$ (Berger 2014), corresponding to a beaming factor $f_b = (1 - \cos \theta_j)^{-1} = 10 - 10^3$.

Short GRBs were found to have comparable beaming factors based on their observed jet breaks and rate (Berger 2014). Nevertheless, the detection of GRB 170817A at a higher observing angle of $\sim 30^\circ \pm 15^\circ$ (Abbott et al. 2018a) implied weaker effective beaming. Radio observations of the GRB’s afterglow indicate that the outflow had a narrowly collimated relativistic jet with $\theta_j < 5^\circ$ as well as a broader, less energetic component (Ghirlanda et al. 2018; Mooley et al. 2018a). The origin of this structured outflow remains the subject of active debate (Haggard et al. 2017; Alexander et al. 2018; Gottlieb et al. 2018; Ioka & Nakamura 2018; Lazzati et al. 2018; Mooley et al. 2018b; Veres et al. 2018).

It is instructive to compare the present limits to previous results. Here, we look at the latest estimates that used Initial LIGO-Virgo and the partially completed IceCube detector (Aartsen et al. 2014a). Considering a fiducial source emission of $E_{\text{GW}} = 10^{-2} M_\odot c^2$ and $E_{\nu, \text{iso}} = 10^{51}$ erg, assuming a beaming factor of $f_b = 10$, this previous search obtained a joint source rate upper limit of $1.1 \times 10^7 \text{ Gpc}^{-3} \text{ yr}^{-1}$. The present search updates this constraint to $4 \times 10^4 \text{ Gpc}^{-3} \text{ yr}^{-1}$, an improvement of more than 2 orders of magnitude.

3.3. Discussion

Here, we briefly review the expected emission parameters of sources of interest, and compare the our rate density constraints to expectations. While our constraints take into account the total emitted energy in both GWs and high-energy neutrinos, and the high-energy beaming factor, the source constraints are also affected by the chosen gravitational waveform and the neutrino spectrum, which we do not explore here in detail. The comparison below should therefore be considered qualitative.

We show in Figure 2 the local ($z = 0$) rate density of core-collapse supernovae (CCSNe) and BNS mergers. The rate of neutron star–black hole mergers, which also could produce relativistic jets, is expected to be lower, $\lesssim 50 \text{ Gpc}^{-3} \text{ yr}^{-1}$ (Gupta et al. 2017). For CCSNe, it is possible that a large fraction of them drive relativistic jets (Piran et al. 2017), potentially resulting in high-energy neutrino emission. Many of these jets may be stalled, however, before they are able to break through the stellar envelope (Mészáros & Waxman 2001; Senno et al. 2016). The resulting choked jets will have no observable gamma-ray emission, making high-energy neutrinos an interesting way to probe them.

For CCSNe, we adopted the local rate of $(7 \pm 3) \times 10^4 \text{ Gpc}^{-3} \text{ yr}^{-1}$ from Li et al. (2011). For BNS mergers, we adopted the rate $1540^{+3200}_{-1220} \text{ Gpc}^{-3} \text{ yr}^{-1}$ obtained from the detection of GW170817 (Abbott et al. 2017d).

The total energy emitted in GWs in BNS mergers is a few percent of a solar mass. It depends on the neutron star masses as well as the nuclear equation of state (Bernuzzi et al. 2016). The expected rate of neutron star–black hole mergers falls below the shown range, while their GW energy could extend beyond $10^{-1} M_\odot c^2$, even for black hole masses $\lesssim 10 M_\odot$, which can disrupt a neutron star upon merger.

The range of E_{GW} is uncertain for CCSNe. Numerical simulations of stellar core-collapse typically predict low GW emission, with $E_{\text{GW}} \lesssim 10^{-7} M_\odot c^2$ (Ott 2009; Yakunin et al. 2010; Kotake et al. 2012; Müller et al. 2013). For core-collapse events with rapidly rotating cores E_{GW} may be boosted to $10^{-2} M_\odot c^2$ if a substantial fraction of the newly formed protoneutron star rotational energy is radiated away in GWs (Fryer et al. 2002; Corsi & Mészáros 2009; Bartos et al. 2013b;

Kashiyama et al. 2016). fallback accretion onto the proto-neutron star can further increase the available angular momentum for GW emission (Piro & Thrane 2012).

High-energy neutrino emission from relativistic jets driven by either CCSNe or BNS mergers is not well understood. For GRBs, the total radiated energy $E_{\nu, \text{iso}}$ can be comparable to the energy radiated in gamma-rays (Waxman & Bahcall 1997), although $E_{\nu, \text{iso}}$ from GRBs has been observationally constrained by the non-detection of coincident neutrinos (Abbasi et al. 2012; Adrián-Martínez et al. 2013b; Aartsen et al. 2017d).

Neutrino emission can be enhanced for sub-photospheric dissipation processes, in which the observable gamma-ray flux is reduced by absorption (Bartos et al. 2013a). A particularly interesting scenario is emission, while the jet is still inside the stellar envelope (Mészáros & Waxman 2001; Razzaque et al. 2003; Bartos et al. 2012; Senno et al. 2016; Tamborra & Ando 2016). As these events are faint or dark in gamma-rays, their $E_{\nu, \text{iso}}$ is not strongly bound by observations as is the case for GRBs.

Recently, there has been significant interest in high-energy neutrino emission from BNS mergers. Kimura et al. (2017a) found that the most promising neutrino sources are GRBs with extended emission that could produce $E_{\nu, \text{iso}} \sim 10^{51}$ erg. Extended emission refers to the weaker X-ray/gamma-ray emission observed for some short GRBs that follow the main short burst, which typically lasts for a hundred seconds. The origin of this emission is currently not understood. Fang & Metzger (2017) investigated the possibility that a long-lived neutron star remnant survives the BNS merger, and calculated the interaction between winds from the remnant with matter ejected from the merger. They found that this interaction could produce neutrinos over a period of weeks to a year that could reach $\sim 10^{50}$ erg energy. This particular emission model is not constrained by the present search due to its expected duration.

Following the discovery of BNS merger GW170817, Biehl et al. (2018) looked at the expected neutrino flux for GRBs with structured jets observed at large viewing angles, finding a low $E_{\nu, \text{iso}} \sim 10^{44}$ erg. Kimura et al. (2018) studied neutrino emission in jets burrowing through the mildly relativistic ejecta of BNS mergers. They found that this trans-ejecta neutrino emission, when viewed on-axis, can reach $E_{\nu, \text{iso}} \sim 10^{51}$ erg.

Binary black hole mergers could also produce electromagnetic and neutrino emission if the black holes reside in a gaseous environment, although this scenario is not expected to arise for the majority of events. The first observational hint for such was the observation of a possible short GRB by the Gamma-ray Burst Monitor on the *Fermi* satellite (Connaughton et al. 2016). Scenarios that can result in electromagnetic and neutrino emission include mergers in the accretion disks of active galactic nuclei (Bartos et al. 2017a, 2017b; Stone et al. 2017), gas, or debris remaining around the black holes from their prior evolution (Kotera & Silk 2016; Moharana et al. 2016; Murase et al. 2016; Perna et al. 2016; de Mink & King 2017; but see Kimura et al. 2017b), and binary black hole formation inside a collapsing star (Loeb 2016; but see Dai et al. 2017). The electromagnetic and neutrino brightness of binary black hole mergers within these scenarios is currently not well constrained. Continued follow-up observations of mergers discovered through GWs in the future will be able to confirm or provide interesting constraints on these models.

4. Conclusion

We searched for joint sources of GWs and high-energy neutrinos using observations from Advanced LIGO during its first observing run O1, and the ANTARES and IceCube neutrino observatories. We identified no significant coincident GW and neutrino candidates.

We used the non-detection to obtain constraints on the rate density of multimessenger GW+neutrino sources as functions of the energy emitted in gravitational waves and neutrinos. For realistic multimessenger source rate densities of $<10^5 \text{ Gpc}^{-3} \text{ yr}^{-1}$, the derived limits are constraining in the strong-emission regime of $E_{\text{GW}} \gtrsim 10^{-2} M_{\odot} c^2$ and $E_{\text{iso},\nu} \gtrsim 10^{51} \text{ erg}$. Such GW brightness is highly optimistic for CCSN events but it is more realistic for the case of compact binary mergers, while such neutrino brightness is comparable to the gamma-ray brightness of GRBs.

The considered observing period had an effective duration of just $\sim 0.13 \text{ yr}$, which will be surpassed by future GW observing runs. In addition, we anticipate that LIGO's sensitivity will improve by a factor of ~ 2 upon reaching design sensitivity (Abbott et al. 2018b). Furthermore, other detectors such as Virgo will be operational in future observing periods (Virgo was partially operational during the second observing run, O2). Meanwhile, planned next-generation neutrino detectors at the South Pole (Aartsen et al. 2014b), the Mediterranean (Adrián-Martínez et al. 2016b) and in Lake Baikal (Avrorin et al. 2018) will lead to similarly significant improvements in sensitivity to high-energy astrophysical neutrinos. In light of these gains, we expect our sensitivity to possible multimessenger GW+neutrino sources to improve significantly in the near future.

The ANTARES Collaboration acknowledge the financial support of the funding agencies: Centre National de la Recherche Scientifique (CNRS), Commissariat à l'énergie atomique et aux énergies alternatives (CEA), Commission Européenne (FEDER fund and Marie Curie Program), Institut Universitaire de France (IUF), IdEx program and UnivEarthS Labex program at Sorbonne Paris Cité (ANR-10-LABX-0023 and ANR-11-IDEX-0005-02), Labex OCEVU (ANR-11-LABX-0060) and the A*MIDEX project (ANR-11-IDEX-0001-02), Région Île-de-France (DIM-ACAV), Région Alsace (contrat CPER), Région Provence-Alpes-Côte d'Azur, Département du Var and Ville de La Seyne-sur-Mer, France; Bundesministerium für Bildung und Forschung (BMBF), Germany; Istituto Nazionale di Fisica Nucleare (INFN), Italy; Nederlandse organisatie voor Wetenschappelijk Onderzoek (NWO), the Netherlands; Council of the President of the Russian Federation for young scientists and leading scientific schools supporting grants, Russia; National Authority for Scientific Research (ANCS), Romania; Ministerio de Economía y Competitividad (MINECO); Plan Estatal de Investigación (refs. FPA2015-65150-C3-1-P, -2-P and -3-P, (MINECO/FEDER)), Severo Ochoa Centre of Excellence and MultiDark Consolider (MINECO), and Prometeo and Grisolia programs (Generalitat Valenciana), Spain; Ministry of Higher Education, Scientific Research and Professional Training, Morocco. We also acknowledge the technical support of Ifremer, AIM and Foselev Marine for the sea operation and the CC-IN2P3 for the computing facilities. The IceCube Collaboration gratefully acknowledges the following support: USA—U.S. National Science Foundation-Office of Polar Programs, U.S. National Science Foundation-Physics Division, Wisconsin Alumni Research Foundation, Center for High Throughput Computing

(CHTC) at the University of Wisconsin-Madison, Open Science Grid (OSG), Extreme Science and Engineering Discovery Environment (XSEDE), U.S. Department of Energy-National Energy Research Scientific Computing Center, Particle astrophysics research computing center at the University of Maryland, Institute for Cyber-Enabled Research at Michigan State University, and Astroparticle physics computational facility at Marquette University; Belgium—Funds for Scientific Research (FRS-FNRS and FWO), FWO Odysseus and Big Science programmes, and Belgian Federal Science Policy Office (Belspo); Germany—Bundesministerium für Bildung und Forschung (BMBF), Deutsche Forschungsgemeinschaft (DFG), Helmholtz Alliance for Astroparticle Physics (HAP), Initiative and Networking Fund of the Helmholtz Association, Deutsches Elektronen Synchrotron (DESY), and High Performance Computing cluster of the RWTH Aachen; Sweden—Swedish Research Council, Swedish Polar Research Secretariat, Swedish National Infrastructure for Computing (SNIC), and Knut and Alice Wallenberg Foundation; Australia—Australian Research Council; Canada—Natural Sciences and Engineering Research Council of Canada, Calcul Québec, Compute Ontario, Canada Foundation for Innovation, WestGrid, and Compute Canada; Denmark—Villum Fonden, Danish National Research Foundation (DNRF); New Zealand—Marsden Fund; Japan—Japan Society for Promotion of Science (JSPS) and Institute for Global Prominent Research (IGPR) of Chiba University; Korea—National Research Foundation of Korea (NRF); Switzerland—Swiss National Science Foundation (SNSF). The LIGO Scientific Collaboration and the Virgo Collaboration gratefully acknowledge the support of the United States National Science Foundation (NSF) for the construction and operation of the LIGO Laboratory and Advanced LIGO as well as the Science and Technology Facilities Council (STFC) of the United Kingdom, the Max-Planck-Society (MPS), and the State of Niedersachsen/Germany for support of the construction of Advanced LIGO and construction and operation of the GEO600 detector. Additional support for Advanced LIGO was provided by the Australian Research Council. The authors gratefully acknowledge the Italian Istituto Nazionale di Fisica Nucleare (INFN), the French Centre National de la Recherche Scientifique (CNRS) and the Foundation for Fundamental Research on Matter supported by the Netherlands Organisation for Scientific Research, for the construction and operation of the Virgo detector and the creation and support of the EGO consortium. The authors also gratefully acknowledge research support from these agencies as well as by the Council of Scientific and Industrial Research of India, the Department of Science and Technology, India, the Science & Engineering Research Board (SERB), India, the Ministry of Human Resource Development, India, the Spanish Agencia Estatal de Investigación, the Vicepresidència i Conselleria d'Innovació Recerca i Turisme and the Conselleria d'Educació i Universitat del Govern de les Illes Balears, the Conselleria d'Educació Investigació Cultura i Esport de la Generalitat Valenciana, the National Science Centre of Poland, the Swiss National Science Foundation (SNSF), the Russian Foundation for Basic Research, the Russian Science Foundation, the European Commission, the European Regional Development Funds (ERDF), the Royal Society, the Scottish Funding Council, the Scottish Universities Physics Alliance, the Hungarian Scientific Research Fund (OTKA), the Lyon Institute of Origins (LIO), the Paris Île-de-France Region, the National Research, Development and Innovation Office Hungary (NKFI), the National Research Foundation of Korea, Industry Canada and

the Province of Ontario through the Ministry of Economic Development and Innovation, the Natural Science and Engineering Research Council Canada, the Canadian Institute for Advanced Research, the Brazilian Ministry of Science, Technology, Innovations, and Communications, the International Center for Theoretical Physics South American Institute for Fundamental Research (ICTP-SAIFR), the Research Grants Council of Hong Kong, the National Natural Science Foundation of China (NSFC), the Leverhulme Trust, the Research Corporation, the Ministry of Science and Technology (MOST), Taiwan and the Kavli Foundation. The authors gratefully acknowledge the support of the NSF, STFC, MPS, INFN, CNRS, and the State of Niedersachsen/Germany for provision of computational resources.

ORCID iDs

B. Baret <https://orcid.org/0000-0001-6064-3858>
 T. Grégoire <https://orcid.org/0000-0001-8711-1456>
 M. Kadler <https://orcid.org/0000-0001-5606-6154>
 O. Kalekin <https://orcid.org/0000-0001-6206-1288>
 U. Katz <https://orcid.org/0000-0002-7063-4418>
 E. Leonora <https://orcid.org/0000-0002-0536-3551>
 A. Marinelli <https://orcid.org/0000-0002-1466-1219>
 R. Mele <https://orcid.org/0000-0002-9165-4231>
 P. Migliozi <https://orcid.org/0000-0001-5497-3594>
 M. Sanguinetti <https://orcid.org/0000-0002-7206-2097>
 M. Spurio <https://orcid.org/0000-0002-8698-3655>
 Th. Stolarczyk <https://orcid.org/0000-0002-0551-7581>
 J. Wilms <https://orcid.org/0000-0003-2065-5410>
 M. Ahlers <https://orcid.org/0000-0003-0709-5631>
 E. Bernardini <https://orcid.org/0000-0003-3108-1141>
 J. J. DeLaunay <https://orcid.org/0000-0001-5229-1995>
 P. Desiati <https://orcid.org/0000-0001-9768-1858>
 G. de Wasseige <https://orcid.org/0000-0002-1010-5100>
 P. A. Evenson <https://orcid.org/0000-0001-7929-810X>
 A. Franckowiak <https://orcid.org/0000-0002-5605-2219>
 J. Gallagher <https://orcid.org/0000-0001-8608-0408>
 T. Glüsenkamp <https://orcid.org/0000-0002-2268-9297>
 M. Huber <https://orcid.org/0000-0003-1059-9603>
 A. Keivani <https://orcid.org/0000-0001-7197-2788>
 M. Santander <https://orcid.org/0000-0001-7297-8217>
 J. Vandenbroucke <https://orcid.org/0000-0002-9867-6548>
 S. Westerhoff <https://orcid.org/0000-0002-1422-7754>
 D. L. Xu <https://orcid.org/0000-0003-1639-8829>
 I. Bartos <https://orcid.org/0000-0001-5607-3637>
 B. Bécsy <https://orcid.org/0000-0003-0909-5563>
 M. Beijger <https://orcid.org/0000-0002-4991-8213>
 S. Bernuzzi <https://orcid.org/0000-0002-2334-0935>
 M. Boer <https://orcid.org/0000-0001-9157-4349>
 R. Ciolfi <https://orcid.org/0000-0003-3140-8933>
 N. Cornish <https://orcid.org/0000-0002-7435-0869>
 A. Corsi <https://orcid.org/0000-0001-8104-3536>
 M. W. Coughlin <https://orcid.org/0000-0002-8262-2924>
 T. Dent <https://orcid.org/0000-0003-1354-7809>
 Z. Doctor <https://orcid.org/0000-0002-2077-4914>
 S. Fairhurst <https://orcid.org/0000-0001-8480-1961>
 B. Farr <https://orcid.org/0000-0002-2916-9200>
 W. M. Farr <https://orcid.org/0000-0003-1540-8562>
 M. Fishbach <https://orcid.org/0000-0002-1980-5293>
 B. Giacomazzo <https://orcid.org/0000-0002-6947-4023>
 A. Grado <https://orcid.org/0000-0002-0501-8256>
 C.-J. Haster <https://orcid.org/0000-0001-8040-9807>

I. S. Heng <https://orcid.org/0000-0002-1977-0019>
 A. M. Holgado <https://orcid.org/0000-0003-4143-8132>
 D. E. Holz <https://orcid.org/0000-0002-0175-5064>
 V. Kalogera <https://orcid.org/0000-0001-9236-5469>
 R. Kashyap <https://orcid.org/0000-0002-5700-282X>
 D. Keitel <https://orcid.org/0000-0002-2824-626X>
 P. D. Lasky <https://orcid.org/0000-0003-3763-1386>
 T. B. Littenberg <https://orcid.org/0000-0002-9574-578X>
 C. O. Lousto <https://orcid.org/0000-0002-6400-9640>
 M. E. Lower <https://orcid.org/0000-0001-9208-0009>
 C. Messick <https://orcid.org/0000-0002-8230-3309>
 N. Mukund <https://orcid.org/0000-0002-8666-9156>
 S. Nissanke <https://orcid.org/0000-0001-6573-7773>
 M. Obergaulinger <https://orcid.org/0000-0001-5664-1382>
 R. O’Shaughnessy <https://orcid.org/0000-0001-5832-8517>
 C. Pankow <https://orcid.org/0000-0002-1128-3662>
 F. Panarale <https://orcid.org/0000-0002-7537-3210>
 M. Pitkin <https://orcid.org/0000-0003-4548-526X>
 Javed Rana <https://orcid.org/0000-0001-5605-1809>
 M. Razzano <https://orcid.org/0000-0003-4825-1629>
 P. M. Ricker <https://orcid.org/0000-0002-5294-0630>
 N. Sarin <https://orcid.org/0000-0003-2700-1030>
 S. P. Stevenson <https://orcid.org/0000-0002-6100-537X>
 C. Talbot <https://orcid.org/0000-0003-2053-5582>
 V. Tiwari <https://orcid.org/0000-0002-1602-4176>
 K. Ueno <https://orcid.org/0000-0003-0424-3045>
 Hang Yu <https://orcid.org/0000-0002-6011-6190>
 M. Zevin <https://orcid.org/0000-0002-0147-0835>

References

- Aab, A., Abreu, P., Aglietta, M., et al. 2015, *NIMPA*, 798, 172
 Aab, A., Abreu, P., Aglietta, M., et al. 2016, *PhRvD*, 94, 122007
 Aartsen, M., Abbasi, R., Abdou, Y., et al. 2013a, *PhRvL*, 111, 021103
 Aartsen, M., Abbasi, R., Abdou, Y., et al. 2013b, *Sci*, 342, 1242856
 Aartsen, M., Ackermann, M., Adams, J., et al. 2014a, *PhRvD*, 90, 102002
 Aartsen, M., Ackermann, M., Adams, J., et al. 2014b, arXiv:1412.5106
 Aartsen, M., Ackermann, M., Adams, J., et al. 2017a, *JInst*, 12, P03012
 Aartsen, M., Ackermann, M., Adams, J., et al. 2017b, *Aph*, 92, 30
 Aartsen, M., Abraham, K., Ackermann, M., et al. 2017c, *ApJ*, 835, 151
 Aartsen, M., Ackermann, M., Adams, J., et al. 2017d, *ApJ*, 843, 112
 Aartsen, M., Ackermann, M., Adams, J., et al. 2018, *Sci*, 361, 147
 Abadie, J., Abbott, B. P., Abbott, R., et al. 2010, *PhRvD*, 81, 102001
 Abadie, J., Abbott, B. P., Abbott, R., et al. 2015, *CQGra*, 32, 074001
 Abbasi, R., Abdou, Y., Abu-Zayyad, T., et al. 2012, *Natur*, 484, 351
 Abbott, B., Abbott, R., Abbott, T. D., et al. 2016a, *PhRvX*, 6, 041015
 Abbott, B., Abbott, R., Abbott, T. D., et al. 2016b, *PhRvD*, 93, 122004
 Abbott, B., Abbott, R., Abbott, T. D., et al. 2017a, *PhRvL*, 118, 221101
 Abbott, B., Abbott, R., Abbott, T. D., et al. 2017b, *ApJL*, 851, L35
 Abbott, B., Abbott, R., Abbott, T. D., et al. 2017c, *PhRvL*, 119, 141101
 Abbott, B., Abbott, R., Abbott, T. D., et al. 2017d, *PhRvL*, 119, 161101
 Abbott, B., Abbott, R., Abbott, T. D., et al. 2017e, *PhRvD*, 95, 042003
 Abbott, B., Abbott, R., Abbott, T. D., et al. 2018a, arXiv:1805.11579
 Abbott, B., Abbott, R., Abbott, T. D., et al. 2018b, *LRR*, 21, 3
 Abe, K., Bronner, C., Hayato, Y., et al. 2018, *ApJL*, 857, L4
 Abe, K., Haga, K., Hayato, Y., et al. 2016, *ApJL*, 830, L11
 Acernese, F., Agathos, M., Agatsuma, K., et al. 2015, *CQGra*, 32, 024001
 Adrián-Martínez, S., Ageron, M., Aguilar, J. A., et al. 2012, *JInst*, 7, T08002
 Adrián-Martínez, S., Ageron, M., Aharonian, F., et al. 2016b, *J. Phys. G*, 43, 084001
 Adrián-Martínez, S., Albert, A., André, M., et al. 2016a, *PhRvD*, 93, 122010
 Adrián-Martínez, S., Al Samarai, I., Albert, A., et al. 2013a, *JCAP*, 6, 008
 Adrián-Martínez, S., Al Samarai, I., Albert, A., et al. 2013b, *A&A*, 559, A9
 Ageron, M., Aguilar, J. A., Al Samarai, I., et al. 2011, *NIMPA*, 656, 11
 Agostini, M., Altenmüller, K., Appel, S., et al. 2017, *ApJ*, 850, 21
 Aguilar, J., Albert, A., Ameli, F., et al. 2007, *NIMPA*, 570, 107
 Aguilar, J., Al Samarai, I., Albert, A., et al. 2011, *Aph*, 34, 539
 Albert, A., André, M., Anghinolfi, M., et al. 2017a, *PhRvD*, 96, 022005
 Albert, A., André, M., Anghinolfi, M., et al. 2017b, *EPJC*, 77, 911

- Albert, A., André, M., Anghinolfi, M., et al. 2017c, *ApJL*, **850**, L35
- Albert, A., André, M., Anghinolfi, M., et al. 2018a, *ApJL*, **853**, L7
- Albert, A., André, M., Anghinolfi, M., et al. 2018b, *ApJL*, **863**, L30
- Alexander, K. D., Margutti, R., Blanchard, P. K., et al. 2018, *ApJL*, **863**, L18
- Avrorin, A. D., Avrorin, A. V., Aynutdinov, V. M., et al. 2018, arXiv:1808.10353
- Baret, B., Bartos, I., Bouhou, B., et al. 2011, *Aph*, **35**, 1
- Baret, B., Bartos, I., Bouhou, B., et al. 2012, *PhRvD*, **85**, 103004
- Bartos, I., Beloborodov, A. M., Hurley, K., & Márka, S. 2013a, *PhRvL*, **110**, 241101
- Bartos, I., Brady, P., & Márka, S. 2013b, *CQGra*, **30**, 123001
- Bartos, I., Dasgupta, B., & Márka, S. 2012, *PhRvD*, **86**, 083007
- Bartos, I., Finley, C., Corsi, A., & Márka, S. 2011, *PhRvL*, **107**, 251101
- Bartos, I., Haiman, Z., Marka, Z., et al. 2017b, *NatCo*, **8**, 831
- Bartos, I., Kocsis, B., Haiman, Z., & Márka, S. 2017a, *ApJ*, **835**, 165
- Beauville, F., Bizouard, M.-A., Blackburn, L., et al. 2008, *CQGra*, **25**, 045002
- Berger, E. 2014, *ARA&A*, **52**, 43
- Bernuzzi, S., Radice, D., Ott, C. D., et al. 2016, *PhRvD*, **94**, 024023
- Biehl, D., Heinze, J., & Winter, W. 2018, *MNRAS*, **476**, 1191
- Connaughton, V., Burns, E., Goldstein, A., et al. 2016, *ApJL*, **826**, L6
- Corsi, A., & Mészáros, P. 2009, *ApJ*, **702**, 1171
- Dai, L., McKinney, J. C., & Miller, M. C. 2017, *MNRAS*, **470**, L92
- de Mink, S. E., & King, A. 2017, *ApJL*, **839**, L7
- Fang, K., & Metzger, B. D. 2017, *ApJ*, **849**, 153
- Fisher, R. 1925, *Statistical Methods for Research Workers* (Edinburgh: Oliver and Boyd)
- Fryer, C. L., Holz, D. E., & Hughes, S. A. 2002, *ApJ*, **565**, 430
- Gando, A., Gando, Y., Hachiya, T., et al. 2016, *ApJL*, **829**, L34
- Ghirlanda, G., Salafia, O. S., Paragi, Z., et al. 2018, arXiv:1808.00469
- Gottlieb, O., Nakar, E., Piran, T., & Hotokezaka, K. 2018, *MNRAS*, **479**, 588
- Gupta, A., Arun, K. G., & Sathyaprakash, B. S. 2017, *ApJL*, **849**, L14
- Haggard, D., Nynka, M., Ruan, J. J., et al. 2017, *ApJL*, **848**, L25
- Halzen, F., & Hooper, D. 2002, *RPPH*, **65**, 1025
- Ioka, K., & Nakamura, T. 2018, *PTEP*, **2018**, 043E02
- Kashiyama, K., Murase, K., Bartos, I., Kiuchi, K., & Margutti, R. 2016, *ApJ*, **818**, 94
- Kimura, S. S., Murase, K., Bartos, I., et al. 2018, arXiv:1805.11613
- Kimura, S. S., Murase, K., Mészáros, P., & Kiuchi, K. 2017a, *ApJL*, **848**, L4
- Kimura, S. S., Takahashi, S. Z., & Toma, K. 2017b, *MNRAS*, **465**, 4406
- Kintscher, T. & the IceCube Collaboration 2016, *JPCS*, **718**, 062029
- Klimenko, S., Vedovato, G., Drago, M., et al. 2011, *PhRvD*, **83**, 102001
- Klimenko, S., Vedovato, G., Drago, M., et al. 2016, *PhRvD*, **93**, 042004
- Klimenko, S., Yakushin, I., Mercer, A., & Mitselmakher, G. 2008, *CQGra*, **25**, 114029
- Kotake, K., Sumiyoshi, K., Yamada, S., et al. 2012, *PTEP*, **2012**, 01A301
- Kotera, K., & Silk, J. 2016, *ApJL*, **823**, L29
- Lazzati, D., Perna, R., Morsony, B. J., et al. 2018, *PhRvL*, **120**, 241103
- Li, W., Chornock, R., Leaman, J., et al. 2011, *MNRAS*, **412**, 1473
- Liang, E., Zhang, B., Virgili, F., & Dai, Z. G. 2007, *ApJ*, **662**, 1111
- Loeb, A. 2016, *ApJL*, **819**, L21
- Loeb, A., & Waxman, E. 2006, *JCAP*, **5**, 003
- Mészáros, P., & Waxman, E. 2001, *PhRvL*, **87**, 171102
- Moharana, R., Razzaque, S., Gupta, N., & Mészáros, P. 2016, *PhRvD*, **93**, 123011
- Mooley, K. P., Deller, A. T., Gottlieb, O., et al. 2018a, *Natur*, **561**, 355
- Mooley, K. P., Nakar, E., Hotokezaka, K., et al. 2018b, *Natur*, **554**, 207
- Müller, B., Janka, H.-T., & Marek, A. 2013, *ApJ*, **766**, 43
- Murase, K., Kashiyama, K., Mészáros, P., Shoemaker, I., & Senno, N. 2016, *ApJL*, **822**, L9
- Ott, C. D. 2009, *CQGra*, **26**, 063001
- Perna, R., Lazzati, D., & Giacomazzo, B. 2016, *ApJL*, **821**, L18
- Piran, T., Nakar, E., Mazzali, P., & Pian, E. 2017, arXiv:1704.08298
- Piro, A. L., & Thrane, E. 2012, *ApJ*, **761**, 63
- Razzaque, S., Mészáros, P., & Waxman, E. 2003, *PhRvD*, **68**, 083001
- Senno, N., Murase, K., & Mészáros, P. 2016, *PhRvD*, **93**, 083003
- Singer, L., Price, L. R., Farr, B., et al. 2014, *ApJ*, **795**, 105
- Stone, N. C., Metzger, B. D., & Haiman, Z. 2017, *MNRAS*, **464**, 946
- Sutton, P. J. 2013, arXiv:1304.0210
- Tamborra, I., & Ando, S. 2016, *PhRvD*, **93**, 053010
- Veres, P., Mészáros, P., Goldstein, A., et al. 2018, arXiv:1802.07328
- Waxman, E., & Bahcall, J. 1997, *PhRvL*, **78**, 2292
- Yakunin, K. N., Marronetti, P., Mezzacappa, A., et al. 2010, *CQGra*, **27**, 194005